„CAROL DAVILA” UNIVERSITY OF MEDICINE AND PHARMACY
BUCHAREST
DOCTORAL SCHOOL
GENERAL MEDICINE

MALALIGNMENT OF THE KNEE EXTENSOR MECHANISM – IMAGING AND SURGICAL CONTRIBUTIONS

THESIS SUMMARY

PhD Supervisor:
PROF. STĂNCULESCU DUMITRU MD MhD

PhD Student:
IACOBESCU LONGIN GEORGIAN MD

2023

Table of contents

Introduction

Lateral patellar instability is a frequent knee injury, predominantly among youngsters and adolescents, with a variable incidence of 6-87 per 100,000 individuals and with multifactorial etiology, the main risk factors being structural anomalies (trochlear dysplasia, TT-TG distance increased over 20 mm, patella alta), but also by demographic factors such as age, studies reporting a higher frequency of this pathology at ages between 18-22 years and female gender [1]. Patients who experience patellar instability are at a high risk of developing recurrent episodes of dislocation, with a recurrence risk of 38 to 72% [2,3].

The management of extensor mechanism malalignments is laborious and difficult in the context of multifactorial etiology. In the case of the first episode of dislocation, the therapeutic attitude remains the conservative treatment, the surgical treatment being reserved for patients who associate osteochondral fragments [3,4]. By comparison, patients with recurrent dislocations will benefit from surgical treatment to reduce the risk of morbidity, represented by pain in the patellofemoral compartment, recurrent instability and finally patellofemoral arthrosis [3,5]. Preoperatively, the patient will undergo a clinical lesion assessment and an imaging evaluation that will include conventional radiographs, computer tomography with axial measurements and advanced nuclear magnetic resonance imaging. The surgical treatment of malalignments of the extensor mechanism is complex and in direct correlation with the associated factors, but also with the increased risk of dislocation recurrence.

The first part of the present PhD research includes the identification of the current state of knowledge, quantifying the methods of diagnosis and treatment of patellofemoral instability and malalignment of the knee extensor mechanism. In recent years, various surgical techniques have been described in literature, such as the reconstruction of the medial patellofemoral ligament, distal realignment of the patellar tendon involving tibial tubercle osteotomies or release of lateral retinaculum. Generally, procedures involving tibial tubercle osteotomies were aimed at correcting the exaggerated Q angle and an increased TT-TG distance that causes patellar maltracking, unwanted loading on the cartilage, incongruence, instability and possible pain. The best-known osteotomy techniques are Elmslie-Trillat, Roux Goldthwait, Fulkerson and Maquet.

One of the main objectives of the PhD thesis is the identification of the correlations between the variables measured by CT with axial measurements and MRI. Another objective is the main etiologies that lead to malalignments of the knee extensor mechanism, the use of new precise and reliable axial measurements necessary to determine the triggering cause of patellar instability and planning an optimal surgical treatment, as well as the application of new computational methods of analysis, such as the finite element method, which allow the most accurate knowledge of the normal and pathological kinematics of the knee extensor mechanism. The modeling will lead to the deepening of current knowledge and the optimization of established surgical treatments to obtain the best possible functional results. Finally, our aim, as established in the current paper, was to approach the design and identification of some surgical guidance devices that will increase the accuracy, precision and reproducibility of the various techniques involving tibial tubercle osteotomies.

The special part presents the results of a clinical study carried out over a period of six years, which evaluates 60 patients pre- and postoperatively, by advanced CT and MRI, as well as conventional radiology. The main parameters determined were TT-TG distance, the congruence angle, the lateral patellofemoral angle, the trochlear angle, the trochlear facet asymmetry, femoral anteversion and tibial torsion, the Caton-Deschamps, Insall-Salvati and Blackburne-Peel indexes, following their correlation with the individual risk factors, the type of surgery chosen and the Kujala, Lysholm and Tegner functional scores, obtained pre- and postoperatively at 3 and 12 months. The study highlighted the importance of knowing and fully understanding the multifactorial etiology of extensor mechanism malalignments with the application of individualized surgical treatment to each patient.

An important research topic in the current PhD thesis was the identification of new types of axial CT measurements, applicable to patients with patellar instability and trochlear dysplasia, to correctly identify the position of the tibial tubercle in the rotational plane. The limitations of the research were the small number of available cases and the heterogeneous distribution of the etiology causing malalignments of the extensor mechanism. The prospects of obtaining the most statistically relevant results can be offered by an increased number of patients included in the study, by carrying out multicenter studies.

I. General Part

This first part of the PhD thesis is made up of 4 chapters that contain information about the knee anatomy, the biomechanics of the knee extensor mechanism, the malalignment of the knee extensor mechanism and the treatment of patellofemoral instability.

The first chapter, titled “Notions of knee anatomy”, refers to the current study, whose structure of interest is the epiphysis of the distal femur. The lower epiphysis is a voluminous structure with a larger transverse axis than the anteroposterior one, the two condyles entering it, structured into medial condyle and lateral condyle, being divergent from anterior to posterior, thus delimiting the intercondylar fossa.

The following chapter summarizes the information regarding the biomechanics of the knee extensor mechanism, as it is necessary to be fully understood, both at the mechanical level and in terms of the complexity of the interaction of the multiple factors involved in the correct functioning of the entire system.

The third chapter discusses the malalignment of the knee extensor mechanism, which can be determined by numerous factors such as acute trauma, chronic ligament laxity, connective tissue pathology, bone malalignment or anatomical predisposing factors [6].

The main subject of the fourth chapter is the treatment of patellofemoral instability, which aims to obtain a painless, stable and functional joint, decreasing the evolution of osteoarthritis. Thus, in this last chapter of the “General Part”, the principles of conservative treatment, surgical treatment, lateral retinaculum release, medial repair, etc. were explained. MPFL reconstruction techniques, patellar height correction, and tibial tubercle osteotomy procedures, such as the Elmslie-Trillat technique and the Fulkerson technique, as well as other surgical techniques, such as the Hugston-Walsh technique and the Maquet technique, have also been described. Trochleoplasty has been described as reserved for patients with severe trochlear dysplasia, since in most cases, mild and moderate dysplasia is well tolerated by the patient and is a demanding technique that offers a variable prognosis [7].

II. Special part

1. Study on the influence of the indexes obtained from the axis measurements made on computed tomography, nuclear magnetic resonance and radiology in patients with malalignment of the knee extensor mechanism

1.1 Introduction

Patellar instability is a condition with an increased incidence among youngsters and a preponderance among women. Apart from the clinical tests that can be performed, imaging investigations with radiographs, computer tomography and, more recently, with magnetic resonance can bring an important contribution in the process of identifying anatomical variants and anomalies that contribute to patellar instability [8,9].

All these criteria and imaging landmarks were developed and used to correctly quantify trochlear morphology, patellar tracking, patellar morphology and patellar height, factors known to have an important correlation with the clinical situation of patellar instabilities. It is considered that they have an indisputable utility in establishing the diagnosis, but, additionally, they will represent the landmarks for a correct surgical indication [10]. Measurements such as the distance between the tibial tubercle and the deepest point of the tibial tuberosity-trochlear groove (TT-TG), the trochlear angle, the congruence angle, the patellar tilt, the Insall-Salvati index, the Caton Deschamps index, the Blackburne-Peel index, etc., but also the most recent measurements, such as lateral trochlear inclination angle, trochlear height and trochlear facet asymmetry, are known and widely used, all with the aim of better understanding and guidance regarding an optimal surgical treatment [11-14].

The aim of the current study was to clarify these current controversies, by comparing the quality and accuracy of the measurements made on the imaging forms, such as classic radiographs, computed tomography and nuclear magnetic resonance imaging, as well as by identifying the existence of statistically relevant correlations between the various measurements and the follow-up of prognosis and functional results by using evaluation scales.

1.2. Materials and methods

As part of the PhD thesis research, a prospective cohort study was carried out, which included 60 patients, and which took place over a period of six years, between 2016 and 2022. The study enrolled patients from the Orthopedics and Traumatology Clinic of Bucharest University Emergency Hospital, obtained the prior approval of the hospital's ethics committee, the informed consent of the patients to be included in the study group, and complied with the international norms regarding the ethics and deontology of scientific research.

In the statistical analysis, data about the patients, such as age, sex, body mass index, personal pathological antecedents and heredo-collateral antecedents, were taken. The screening of the patients involved performing preoperative and postoperative radiographs of the face, profile and Merchant incidence. All the patients were evaluated preoperatively by computed tomography, with bilateral axial measurements and MRI of the affected knee. The pre- and postoperative functional assessment scales, Kujala, Lysholm and Tegner, were used at 3 months.

The statistical analysis was performed using the IBM SPSS Statistics program version 21. The statistical tests used in the analysis were: the Mann-Whitney U test, the Wilcoxon test and the Chi-Square test. The Phi correlation coefficient was used to identify associations between two dichotomous variables with values between -1 and 1. Cramer's V correlation coefficient measured the strength of association between variables and had values between 0 and +1. The Pearson coefficient measured the strength and direction of the linear relationship between two continuous variables. The Spearman correlation index measured the strength and direction of the link between two continuous variables, two ordinal variables, or between a continuous and an ordinal variable.

1.3 Results

The patients' ages were between 18 and 41 years, half of them being over 25 years old. The average age of the patients was 25.57 years.

Application of the Wilcoxon signed-rank test indicated that there was a statistically significant improvement in the Kujala score measured postoperatively compared to the measurement performed preoperatively ($Z = -6.740$, $p<0.001$) (Graph 1).

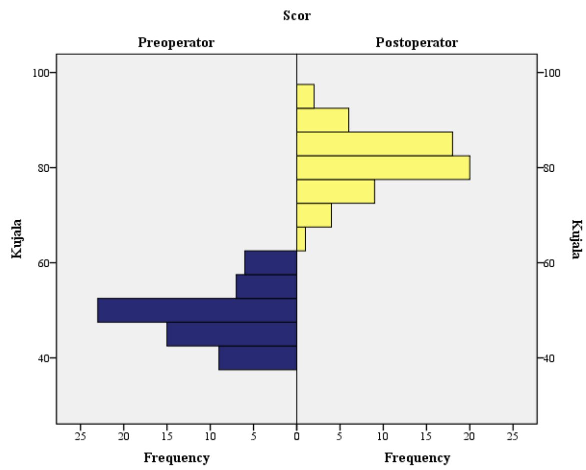

Graph 1. Distribution of cases according to preoperative and postoperative Kujala score

Application of the Wilcoxon signed-rank test indicated that there was a statistically significant improvement in the Lysholm score measured postoperatively compared to the measurement performed preoperatively (Z = -6.747, p<0.001) (Graphs 2, 3).

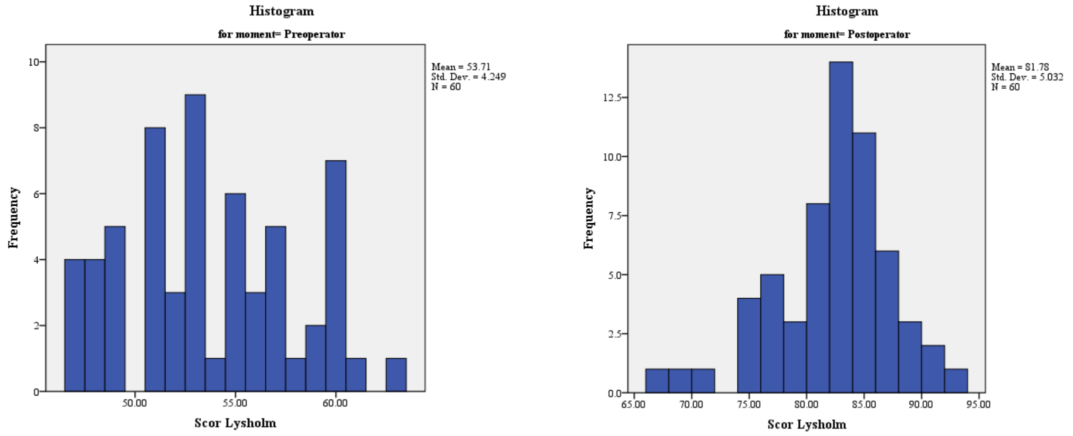

Graphs 2, 3. Distribution of cases according to preoperative and postoperative Lysholm score

Application of the Wilcoxon signed-rank test indicated that there was a statistically significant improvement in the Tegner score measured postoperatively compared to the preoperative measurement (Z = -6.742, p<0.001) (Graph 4).

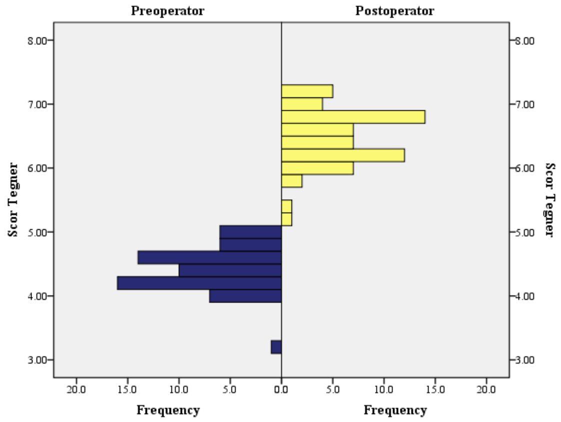

Graph 4. Distribution of cases according to preoperative and postoperative Tegner score

However, the influence of age was noted regarding the scores measured postoperatively, with patients over 30 years of age having significantly lower functional results compared to those under 30 years of age (Graphs 5, 6).

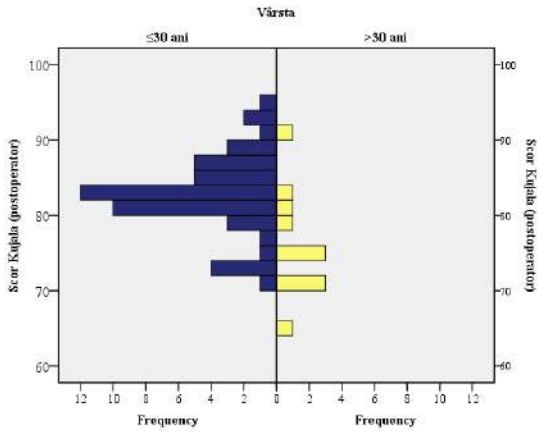

Graph 5. Distribution of cases according to postoperative Kujala score and patients' age

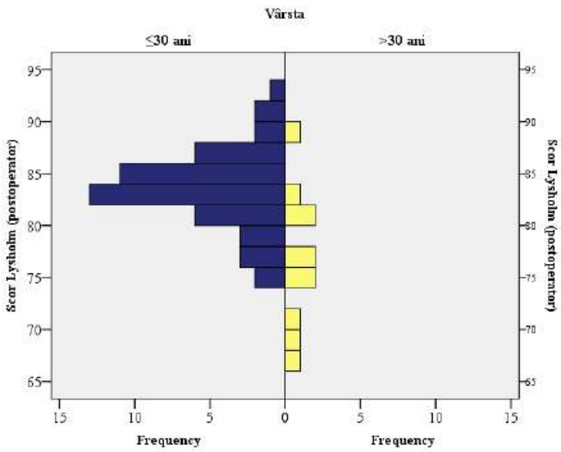

Graph 6. Distribution of cases according to postoperative Lysholm score and patients' age

Functional scores measured preoperatively did not show significant differences in patients with BMI ≤ 30 compared to patients with BMI > 30. Postoperatively, however, significant decreases in functional scores were noted among patients with BMI > 30 compared to patients with BMI ≤ 30 (Graph 7).

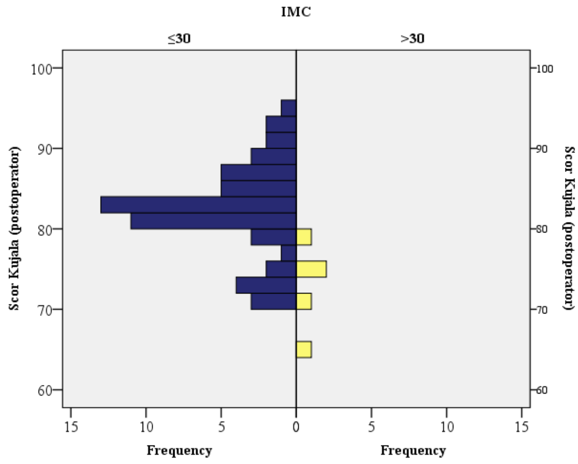

Graph 7. Distribution of cases according to postoperative Kujala score and BMI

Through Spearman correlations, a negative (indirect) but weak correlation was obtained between the postoperative Lysholm score and BMI, rs(58) = -0.255, p=0.049, so it can be argued that the postoperative Lysholm score was decreasing as patients had a higher BMI (Graph 8).

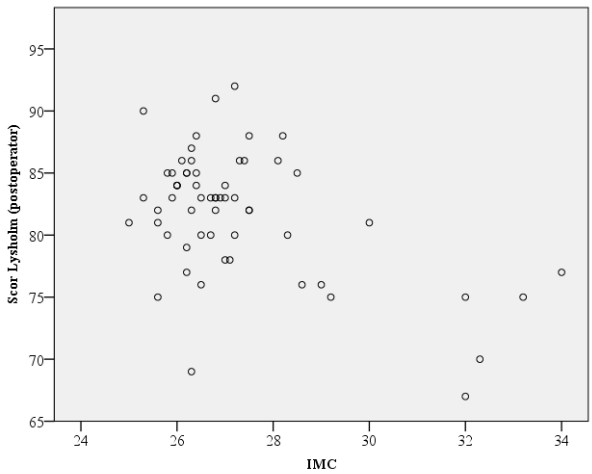

Graph 8. Pearson correlation between postoperative Lysholm score and BMI

Application of the Wilcoxon signed-rank test indicated that there was a statistically significant improvement in the patellar tilt that was measured postoperatively compared to the measurement performed preoperatively (Z = -4.633, p<0.001) (Graph 9).

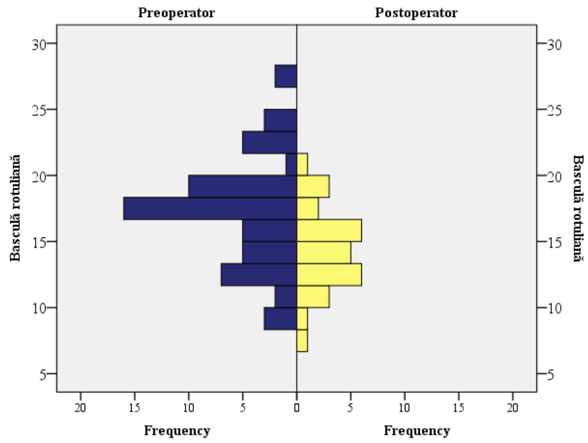

Graph 9. Distribution of cases according to preoperative and postoperative patellar tilt values

Application of the Wilcoxon signed-rank test indicated that there was a statistically significant improvement in the congruence angle measured postoperatively compared to the preoperative measurement ($Z = -4.567$, $p<0.001$) (Graph 10).

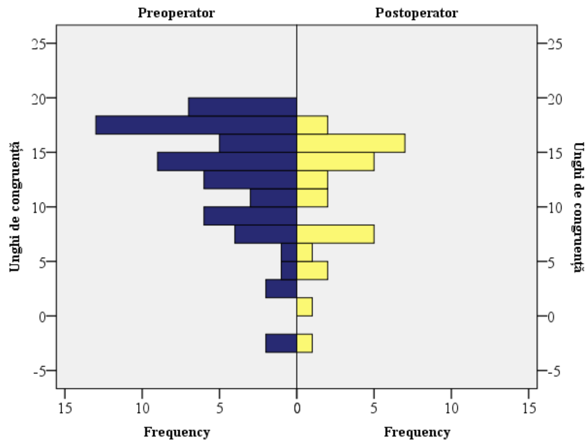

Graph 10. Distribution of cases according to the congruence angle measured preoperatively and postoperatively

Application of the Wilcoxon signed-rank test indicated that there were significant differences between the CD index measured on CT and the CD index measured on MRI ($Z = -5.055$, $p<0.001$) (Graph 11).

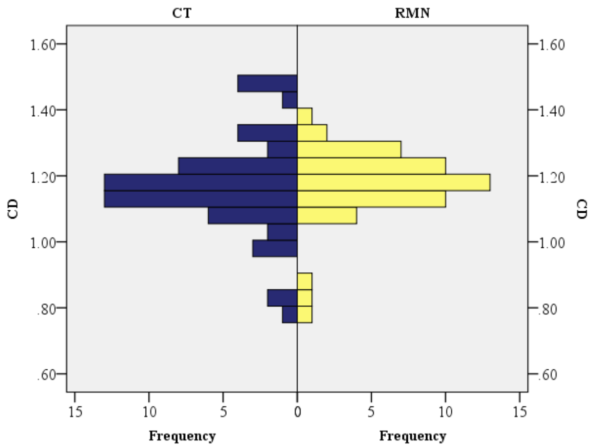

Graph 11. Distribution of cases according to the value of the CD parameter

Application of the Wilcoxon signed-rank test indicated that there were significant differences between trochlear depth measured on CT and trochlear depth measured on X-ray (Z = –3.090, p=0.002) (Graph 12).

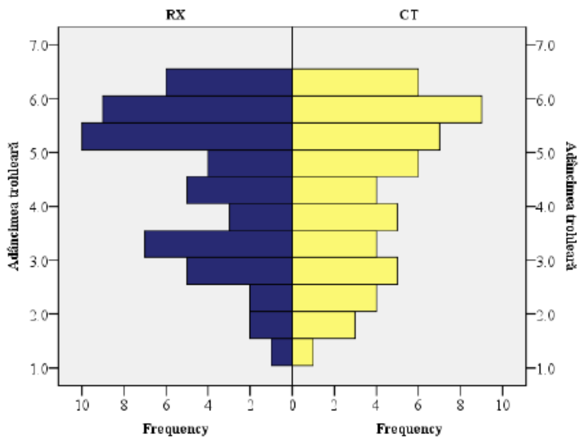

Graph 12. Distribution of cases according to trochlear depth

Application of the Wilcoxon signed-rank test indicated that there were significant differences between the trochlear angle measured on CT and the trochlear angle measured on X-ray (Z = –5.755, p<0.001) (Graph 13).

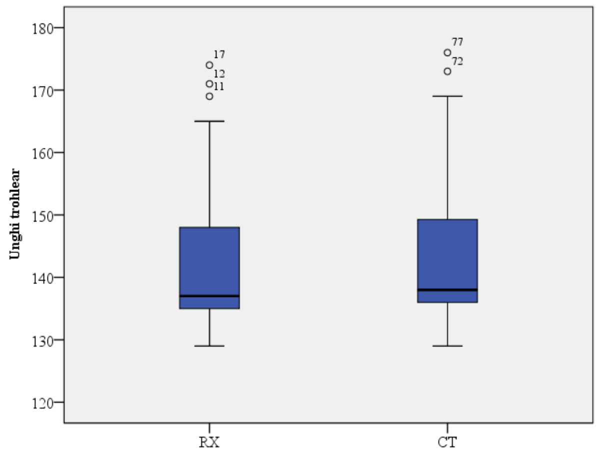

Graph 13. Distribution of cases according to the trochlear angle

Application of the Wilcoxon signed-rank test indicated that there were significant differences between the congruence angle measured on CT and the congruence angle measured on X-ray ($Z = -5.413$, $p<0.001$) (Graph 14).

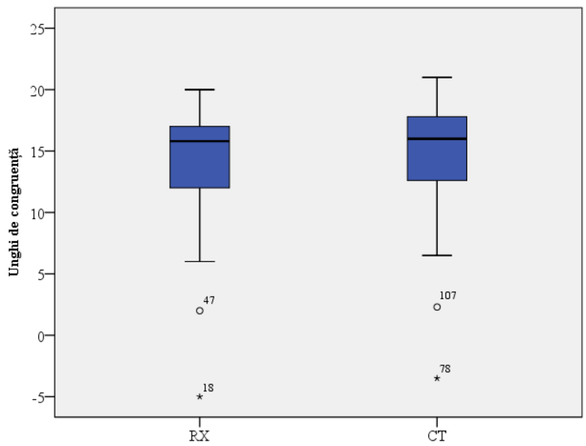

Graph 14. Distribution of cases according to the congruence angle

1.4 Discussions

The aim of the study was to observe the correlation between the axial measurements made by computed tomography, magnetic resonance and conventional radiography with the anatomical anomalies that influenced the occurrence of patellar instabilities, the type of operation performed and the functional results obtained.

Regarding the preoperative symptoms, 85% presented for the clinical situation of patellar instability, having more than 3 recurrent episodes of dislocation. All patients had improved postoperative functional scores, with higher values in patients under 30 years of age and similarly higher values in those with a BMI < 30. Increased BMI also contributed to lower functional scale values.

Statistically significant differences were found between the Kujala score values in patients with TT medialization (Elmsile-Trillat) (mean rank 21.00) and the Kujala score values in ET+MPFL patients (mean rank 44.50), U=246,000, Z=3,940, $p \leq 0.001$. This statistical test indicated that patients with ET+MPFL had a significantly improved postoperative Kujala score compared to patients with TT medialization (Elmsile-Trillat). Similar values were found in the case of the Tegner and Lysholm scores.

TT-TG measurements had higher values on CT compared to MRI, which confirmed the fidelity of CT with axial measurements for this parameter. Similarly, the parameters that quantified the patellar height had variable values during measurements, with correspondence of higher values as follows: IS-CT, CD-MRN and BP similar to CT and MRI.

The study presented several limitations, the first being the small number of patients due to the low incidence of the analyzed pathology among the general population. The heterogeneity and complexity of the risk factors that contributed to patellar instabilities made the statistical analyzes face limitations and difficulties in finding the most relevant correlations.

Another limitation can be that the patients included in the study group benefited from the surgical treatment by several operators. Although there are well-established treatment protocols and standards, the surgical procedure may have a small degree of intraoperative variability. This may influence to some extent the functional results and complications, if present.

The complexity of the variables measured on CT and MRI and the fact that the radiology specialist who analyzed and quantified the measurements was not the same for all patient investigations can also alter the fidelity and accuracy of these measurements.

1.5 Conclusions

It is necessary for patients with pathology of the patellofemoral joint to benefit from the complete radiology screening represented by radiography, computer tomography and nuclear magnetic resonance with axial measurements. A good knowledge of the biomechanics and kinetics of the knee extensor mechanism and the risk factors that lead to the appearance of patellar instabilities, as well as the understanding of the correlations that arise between all these measurements and the structural anatomical anomalies are also essential conditions in applying an optimal surgical treatment [15,16].

2. Numerical analysis, using the Finite Element Method - FEM, for the biomechanics of the knee extensor mechanism

2.1 Introduction

The current study proposed the creation of a kinematic model of the knee extensor mechanism and the identification of the biomechanical consequences that occur in various pathological situations in the patellofemoral joint. An attempt was made to obtain information regarding the stresses and pressure values, which occurred at the interface between the patella and the femur in various degrees of flexion in a normal biomechanical alignment, as well as in the situation of a degree of malalignment through the lateralization of the tibial tubercle.

The situations in which different stages of trochlear dysplasia, also found in the clinical group of patients included in the study, represented by various degrees of lateral trochlear inclination, can lead to blocking of the entire ensemble under analysis, were tested. In the mathematical model used, the situation of joint blockage had a counterpart in orthopedic clinical practice with the situation of a lateral patellofemoral dislocation. The identification of the factors that led to joint blockage, as well as the situations in which tension forces and stress at the patellofemoral contact interface had increased values compared to normal, helped prevent the evolution of premature wear of the joint cartilage resulting in patellofemoral arthrosis. The finite element method was used for the quantification and identification of these values in this experimental study.

2.2 Basic concepts of the finite element method

The finite element method (FEM) presents multiple beneficial characteristics, among which is the ease of the fundamental principles, from which derives its extensive use and applicability. In the discussion about the analysis and modeling of various assemblies with the finite element analysis (FEA), the working assumptions must be correctly and completely understood. If they are not fully understood and applied correctly, we will be exposed to multiple errors in calculation systems and results. Thus, the fundamental principles of FEM were presented.

2.3 The advantages, disadvantages and limits of the finite element method

The advantages of FEM

A rapid expansion in the usual practice, in an extremely low time interval, is a premise for the efficient use of FEM. Some of the most important advantages of the method are: generality, flexibility, simplicity of basic concepts, the use of computers, the existence of FEM calculation programs, pre- and post-processing facilities, the stability of calculation algorithms [17].

The disadvantages of FEM

The excessive extension of FEM and FEA to an increased number of users, without an automatic imposition of a predetermined competence or specialization, makes this method also have certain limitations and clear disadvantages that must be considered. These are represented by the following characteristics: the method is approximate, the calculation model is subjective and arbitrary, the development of the calculation model is laborious, FEM programs are complex and expensive.

2.4 The calculation model and its importance in computer aided-engineering

Creating a model is the first stage in the attempt to abstract from an observable phenomenon, to create an explanatory theory and to anticipate its evolution.

The models encountered in science and technology are logical-mathematical systems or elements with the help of which the properties, behavior in certain given conditions and the evolution of other more complex systems can be indirectly studied. The model represents only a simplification, a partial reflection of the original phenomenon or object [18,19].

Models for engineering calculations in general, therefore also those with finite elements, are approximate mathematical models of the studied structures. There are no general algorithms and methods that guarantee the creation of a unique model [19].

2.5 Modeling in the biomechanics of the human osteoarticular system

Analysis of the modeling of human bone structures using finite element analysis (FEA) requires the use of spatial concepts. Bone structures have difficult and complex geometric correspondences. Thus, it will be necessary to simplify these forms to more natural ones. The reproduction and modeling is done by using the biological material from the corpses.

3. Comparative study on the mechanical behavior of the patellofemoral joint system for cases of malalignment of the knee extensor mechanism and trochlear dysplasia

The study carried out analyzed the evaluation of the biomechanical behavior of the patellofemoral-tibial assembly (knee extensor mechanism) by determining the state of tension and deformation of the patellofemoral joint system. To determine the mechanical behavior, two situations (cases) were analyzed, one that considered the patellofemoral joint system as native (for a healthy organism), and the second one that considered the patellofemoral joint system as modified or pathological through malalignment from the normal biomechanical axis. For the two cases stated, the situations in which the presence of a trochlear dysplasia identified in the study by three degrees of inclination of the lateral trochlear slope led to changes in the kinetics, stress and biomechanics of the patellofemoral joint, were simulated.

The aim of the study was to establish the state of stress in the entire analyzed model, as well as to establish the loading at the contact between the patella and the femur. For these reasons, an equivalent model was created, which simulated the patellofemoral-tibial assembly, analyzing the flexion movement at various degrees, namely 30^o, 60^o, respectively 90^o. The equivalent geometric models of the joint system of the knee were made in the graphic design module of the ANSYS program, in which the numerical simulations were performed.

- ✓ **Case A -** the femur-patella-tibia joint system through the tibial tubercle aligned according to the biomechanical axis;

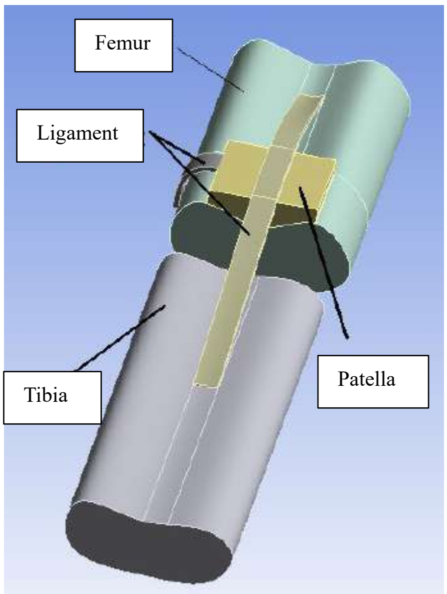

Fig. 1 Kit for **Case A**

- ✓ **Case B -** the femur-patella-tibia joint system deviated laterally from the biomechanical axis through the tibial tubercle;

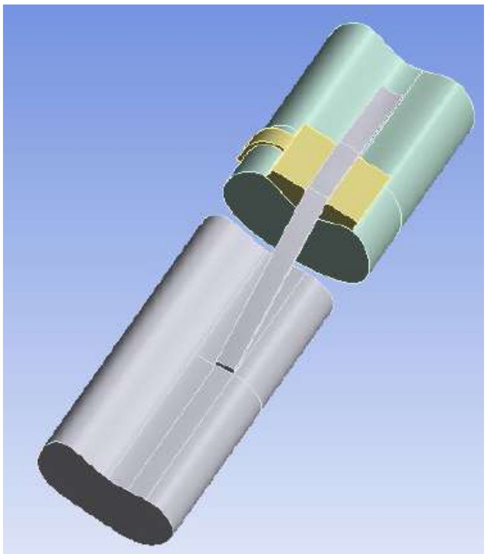

Fig. 2 Kit for **Case B**

Depending on the lateral-trochlear inclination angle, three variants were analyzed for the two configurations, situations exemplified in the schematizations from table 1.

Table 1. Variation of the lateral-trochlear inclination angle

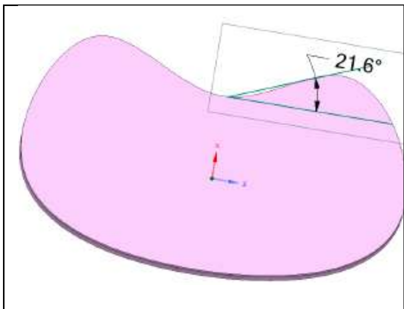	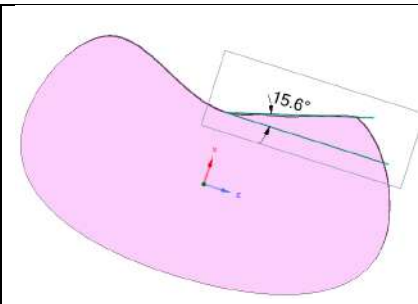	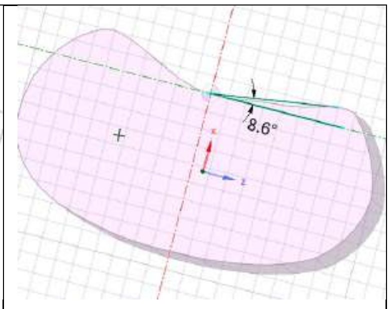
Case A,B - 1	Case A,B - 2	Case A,B - 3

3.1 Creation of the numerical model

In case of performing a numerical analysis using the finite element method, the creation of the numerical model is composed of the following:

- ***The existence of a geometric model***;

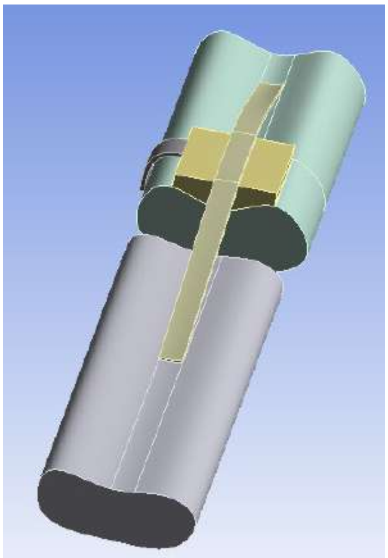

Fig. 3 **Case A** – geometric model

- ***Application of contacts between the components of the assembly created***. For the model made in this study, fixed (Bonded) contacts were applied between the geometric components, without friction between them for the links between the ligaments and the cortical bone tissue, and Frictional contact was applied between the patella and the femur, the coefficient of friction considered being 0.02;

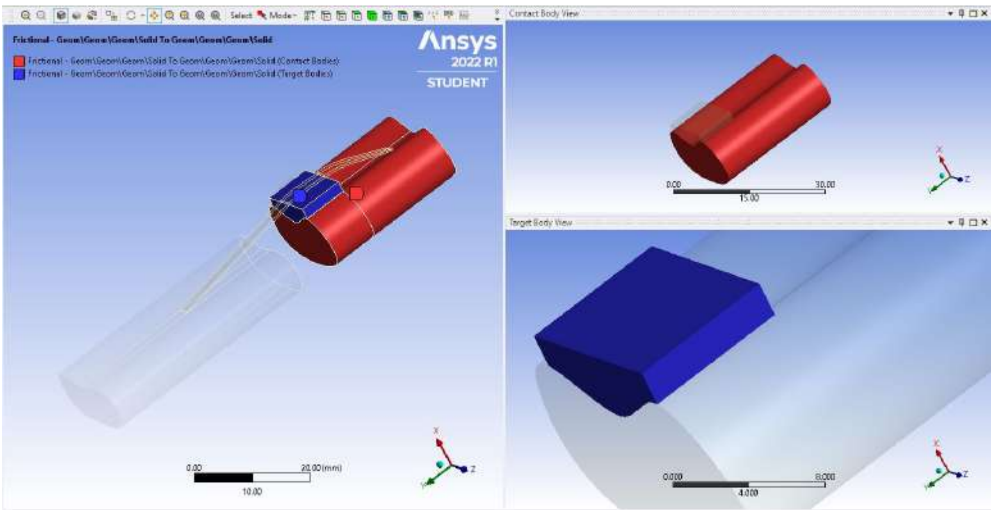

Fig. 4 Defining the contact between the patella and the femur

- ***Analysis model discretization.***

The discretization process involves dividing the geometric components into networks of finite elements interconnected by means of corner or side nodes, so that following the numerical simulation, information is obtained from as many areas as possible in the entire model. As the geometric model was represented three-dimensionally, consisting of solid bodies as volumes, the finite elements used for the discretization process were three-dimensional type elements (SOLID 187).

Due to the contacts that appeared between the components of the assembly, two more types of connecting elements were chosen (elements that mathematically transposed the contact properties), namely CONTA and TARGE elements.

The geometries of these types of finite elements are presented in fig. 5-7.

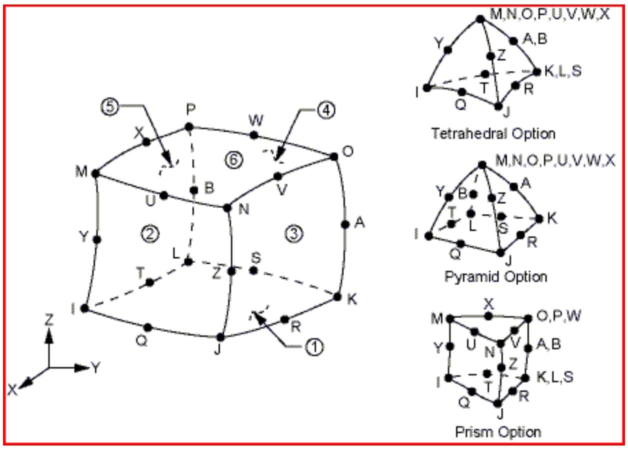

Fig. 5 SOLID 187 finite element geometry

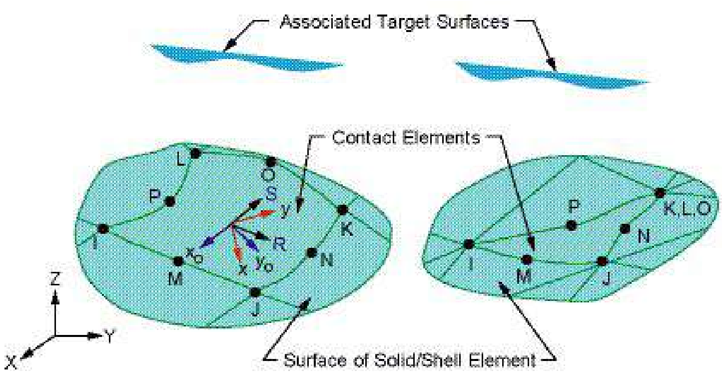

Fig. 6 CONTA 174 finite element geometry

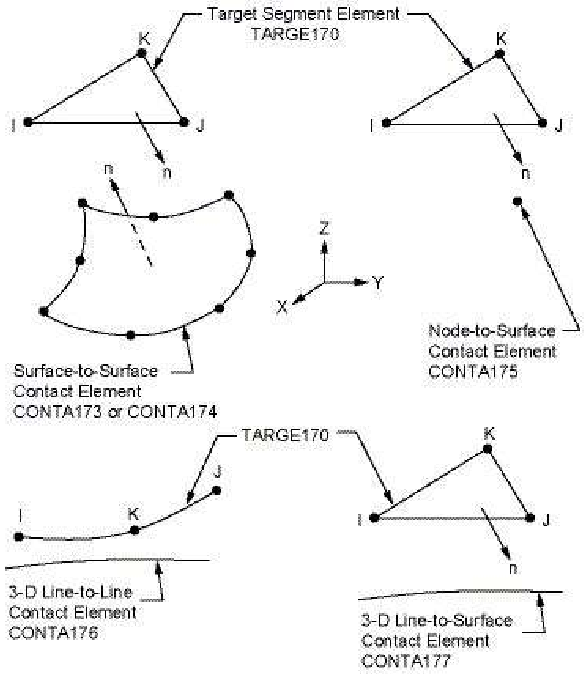

Fig. 7 TARGE 170 finite element geometry

After performing the discretization process, the entire model was divided into a finite element network with a size of 2 mm, consisting of 9917 nodes and 2755 elements.

Fig. 8 shows the discretized geometric model for case A.

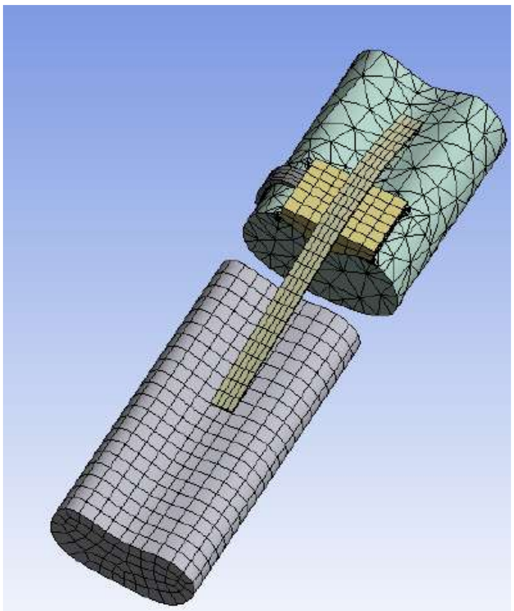

Details of "Mesh"	
Display	
Display Style	Use Geometry Setting
Defaults	
Physics Preference	Mechanical
Element Order	Program Controlled
Element Size	2.0 mm
Sizing	
Quality	
Inflation	
Advanced	
Statistics	
Nodes	9917
Elements	2755

Fig. 8 The discrete finite elements network - **Case A**

- ***Assigning the elastic and mechanical material properties*** for each component of the studied assembly.

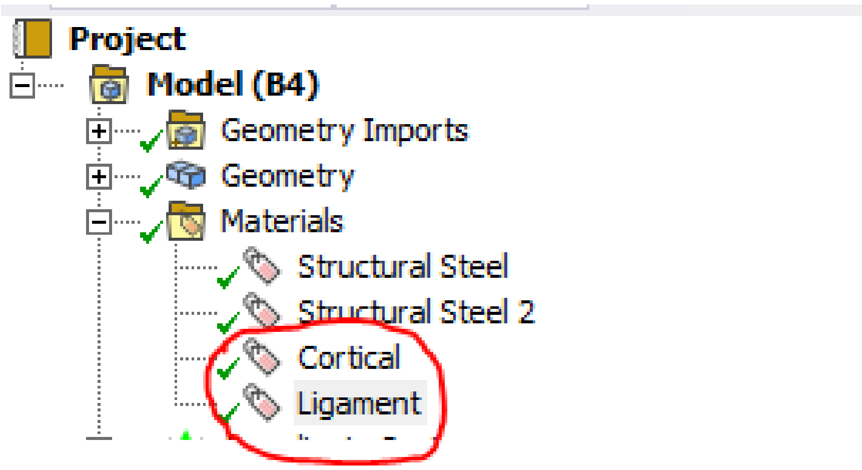

Fig. 9 The materials used in the numerical simulation

Engineering Data: Material View

Cortical

Structural

Isotropic Elasticity	
Derive from	Young's Modulus and Poisson's Ratio
Young's Modulus	24100 MPa
Poisson's Ratio	0.28
Bulk Modulus	18258 MPa
Shear Modulus	9414.1 MPa

Fig. 10 Elastic properties - cortical tissue

Engineering Data: Material View

Ligament

Structural

Isotropic Elasticity	
Derive from	Young's Modulus and Poisson's Ratio
Young's Modulus	10 MPa
Poisson's Ratio	0.47
Bulk Modulus	55.556 MPa
Shear Modulus	3.4014 MPa

Fig. 11 Ligament elastic properties

➢ ***Establishing the way of applying external loads and blockages*** for the studied model.

The aim was to determine the mechanical behavior of the patellofemoral joint system, so that in various positions of the lower limb, depending on the flexion angle, the patellofemoral joint works in balance, and the bone components are aligned along the biomechanical axis, as loading (external load) or displacement (translation) applied to the tibia.

Table 2. Displacement values, depending on the flexion angle

α, [^{0})	30^0	60^0	90^0
w, [mm]	23,63	70,86	240

For the blocking mode of the model, the type of blocking on the outer surface, in the lower part of the model, was chosen, considering it as a fixed type blocking, without any degree of freedom (all six possible movements being cancelled).

Blockage A represented the "Fixed" connection, which was applied considering that the patient was in a sitting position; the "Remote displacement" type C connection was applied to the face of the body considered the tibial bone, canceling the lateral translations; the rotational movement around the OZ axis was free, and B represented a displacement-type constraint; the displacements were canceled along the OZ and OY axes, and the displacements calculated in table 2 were applied in the direction of the OX axis.

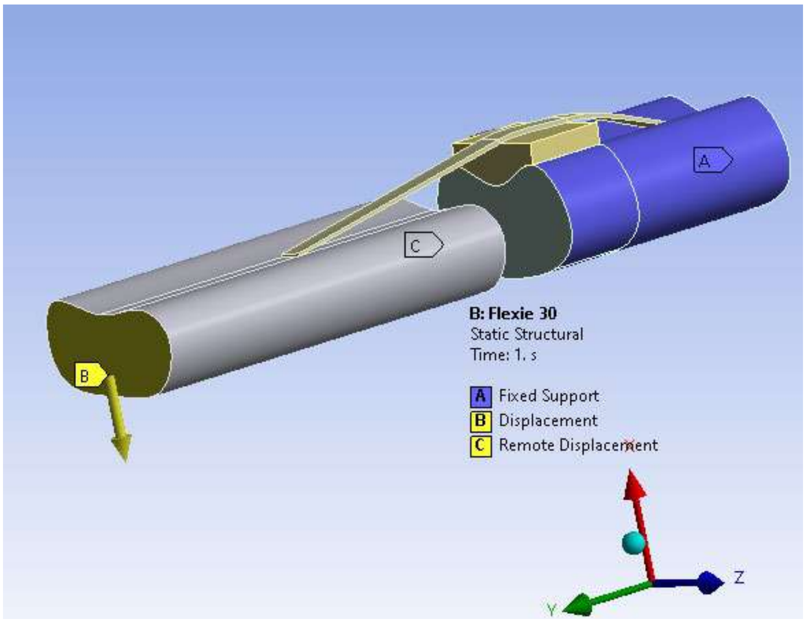

Fig. 12 Loading and blockages application method - **Case A**

- ***Solving (Solution) of the created numerical model***

After completing all the stages listed above, the type of analysis was selected and the solution module was activated, and then, after reaching convergence, the results set for solving were displayed.

3.2 Results

1. ***Case A - variants 1, 2 și 3*** - the patellofemoral joint system aligned along the biomechanical axis

In the following, the results obtained from the numerical calculation performed for **Case A** were presented, which aimed to determine the contact pressure at the interface between the elements of the patellofemoral joint system.

Fig. 13 shows the variation of the total (equivalent) displacement in the entire assembly, for the three degrees of flexion analyzed. A distribution from distal to proximal of the equivalent displacement zones of the assembly is observed.

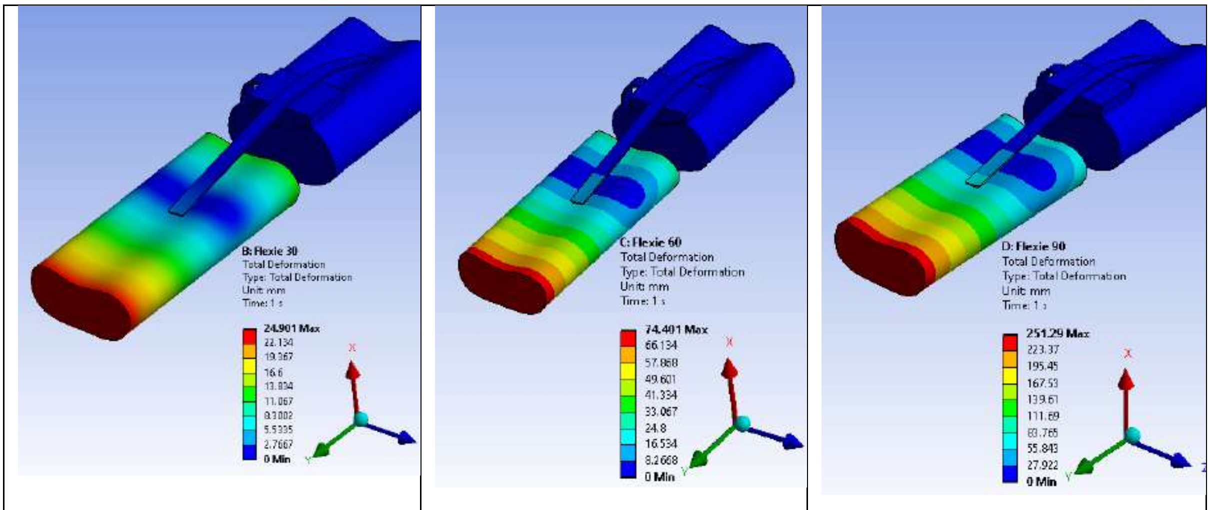

Flexion 30º	Flexion 60º	Flexion 90º

Fig. 13 Variation of the equivalent displacement in the model

Fig. 14 shows the distribution of the equivalent stress in the assembly, determined according to the von Mises criterion for the Flexion movement at 30º.

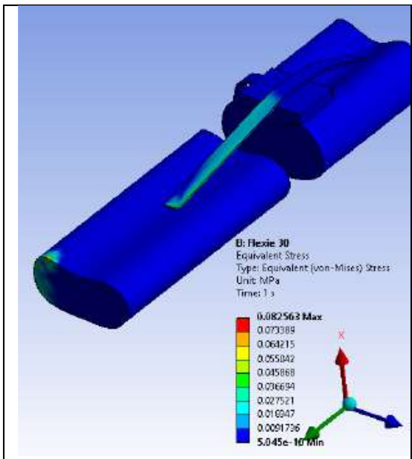	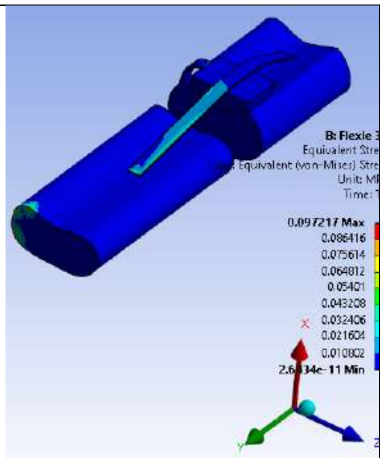	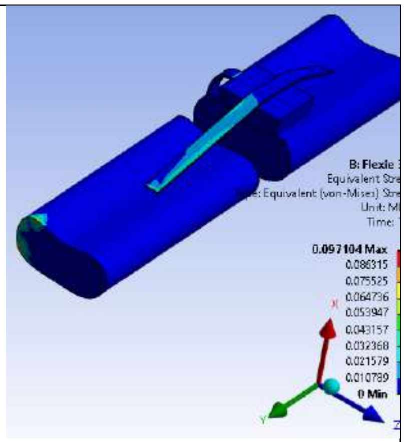
Case A-1	Case A-2	Case A-3

Fig. 14 Variation of the equivalent stress in the model - Flexion 30º

Analyzing fig. 15, it can be concluded that the variation of the equivalent stress increases with the decrease of the angle of lateral trochlear inclination.

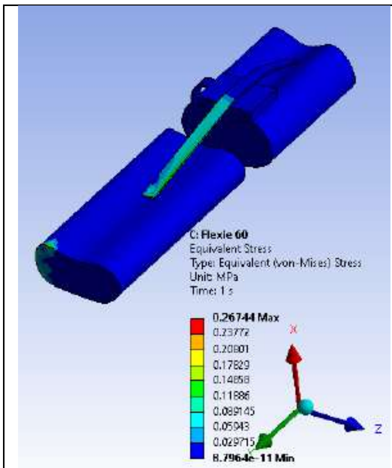	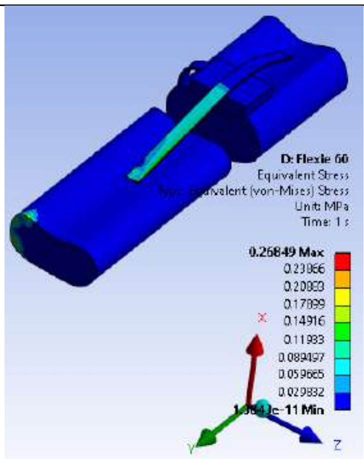	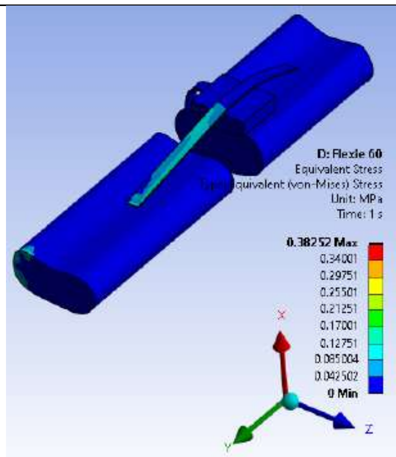
Case A-1	Case A-2	Case A-3

Fig. 15 Variation of the equivalent stress in the model - Flexion 60º

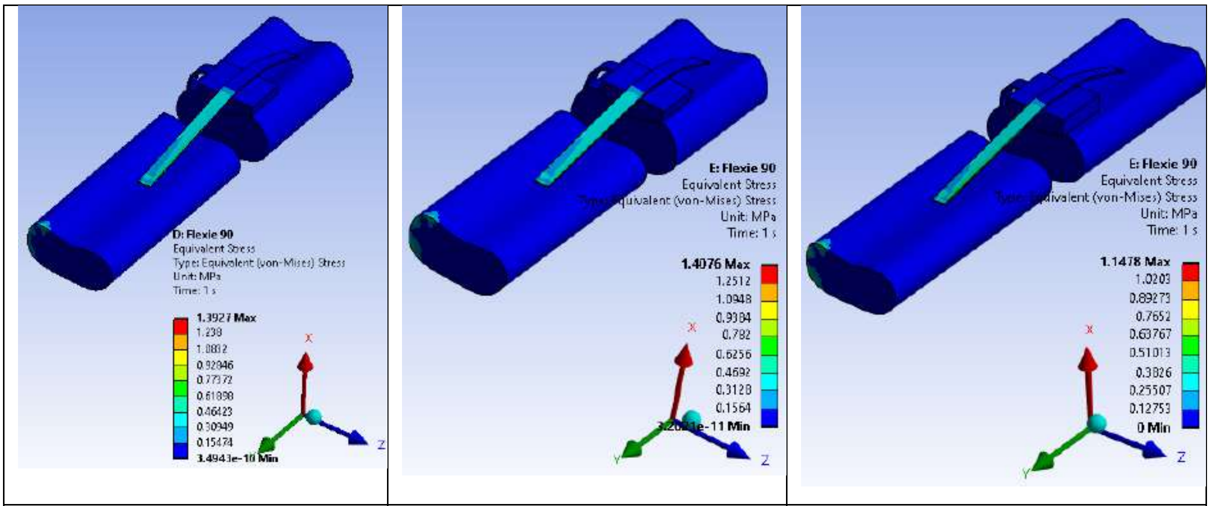

Case A-1	Case A-2	Case A-3

Fig. 16 Variation of the equivalent stress in the model - Flexion 90º

The same biomechanical finding was observed in fig. 15 and 16 and was valid for flexion of 60º and 90º, in which the variation of the equivalent stress increased with the decrease of the angle of lateral trochlear inclination.

Fig. 17 shows the movement of the connected components.

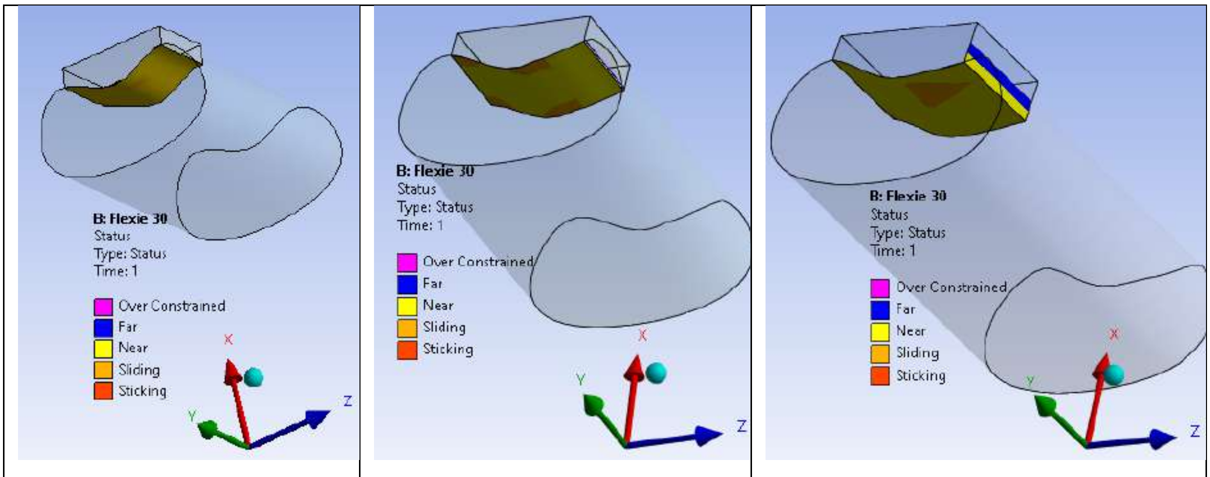

Case A-1	Case A-2	Case A-3

Fig. 17 Control elements in the patellofemoral contact area - Flexion 30º

As anticipated, analyzing fig. 17, the contact between the two components, the femur on the one hand and the patella on the other, being characterized by friction, it was found that there was a sliding between the two components, which corresponded to the real functioning of the joint. For variant A-3, it was observed that there was a sliding of the patella from the central axis to the lateral part of the knee joint, which led to the conclusion that in this situation the phenomenon of joint locking could occur. The stress of the medial connecting structure, represented by the MPFL, was taken over due to the lack of stabilization, through the modified anatomical architecture of the lateral trochlear slope.

The presentation of the control elements of the contact between the two components had the role of observing the phenomena that appear at the interface between them following the movements that were transmitted in the contact area, being also a tool for checking the way in which the analiyed structure was modeled.

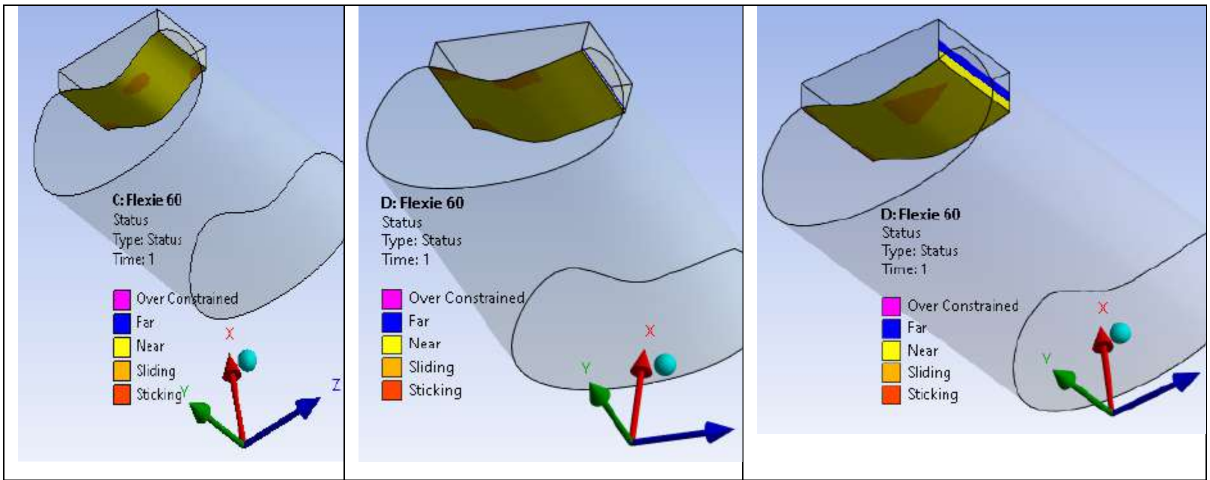

Case A-1	Case A-2	Case A-3

Fig. 18 Control elements in the patellofemoral contact area - Flexion 60º

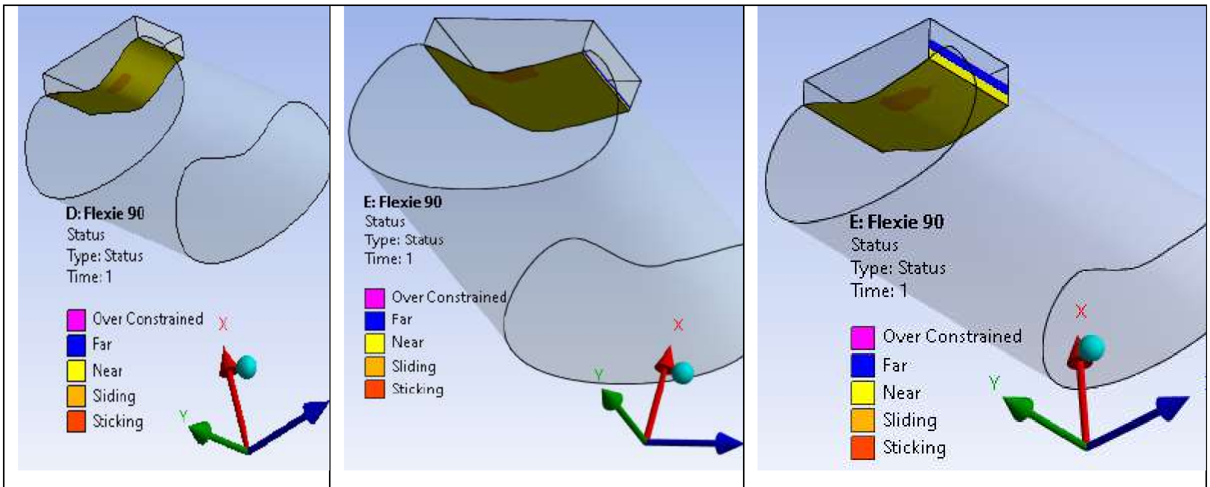

Case A-1	Case A-2	Case A-3

Fig. 19 Control elements in the patellofemoral contact area - 90º flexion

Analyzing fig. 17-19, it was found that the sliding area between the two bodies (patellofemoral joint) increased as the degree of flexion increased, which could have led to the appearance of the phenomenon of instability of the assembly.

Fig. 20 shows the stress variation at the interface between the two connected components.

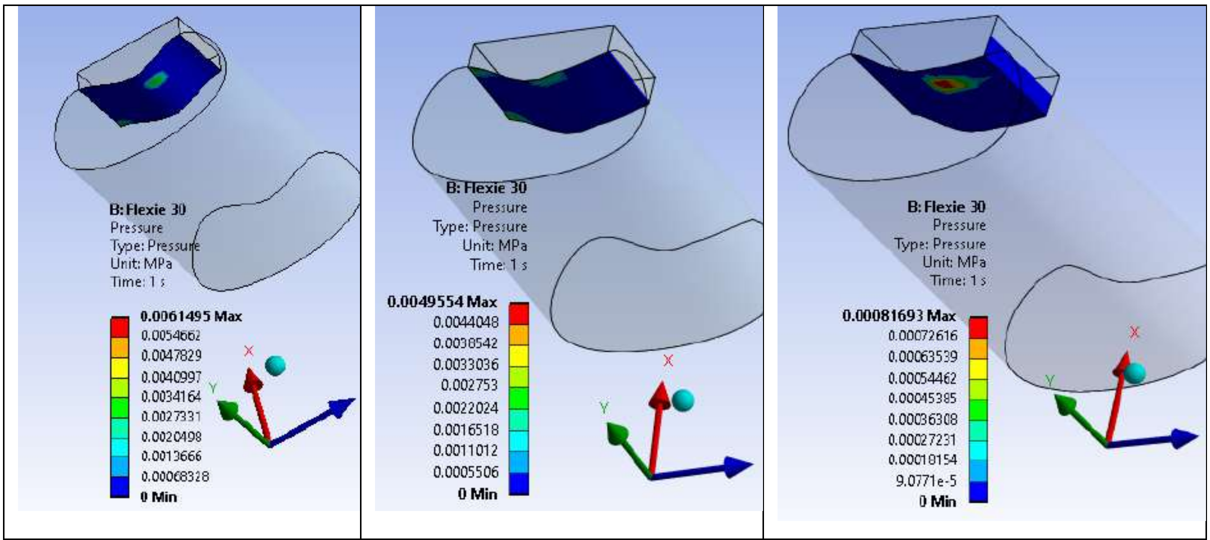

Case A-1	Case A-2	Case A-3

Fig. 20 Stress variation in the contact area - Flexion 30º

The stress variation in the contact area is a very important component in the analysis of the elements, because a stress (reaching high values of the contact stress relative to the contact surface) of the contact area can explain the occurrence of chondropathy and later arthrosis of the patellofemoral joint. The analysis revealed that more flexion relative to a smaller lateral trochlear inclination angle leads to an increased contact area, but with a lower stress value, due to an extended distribution.

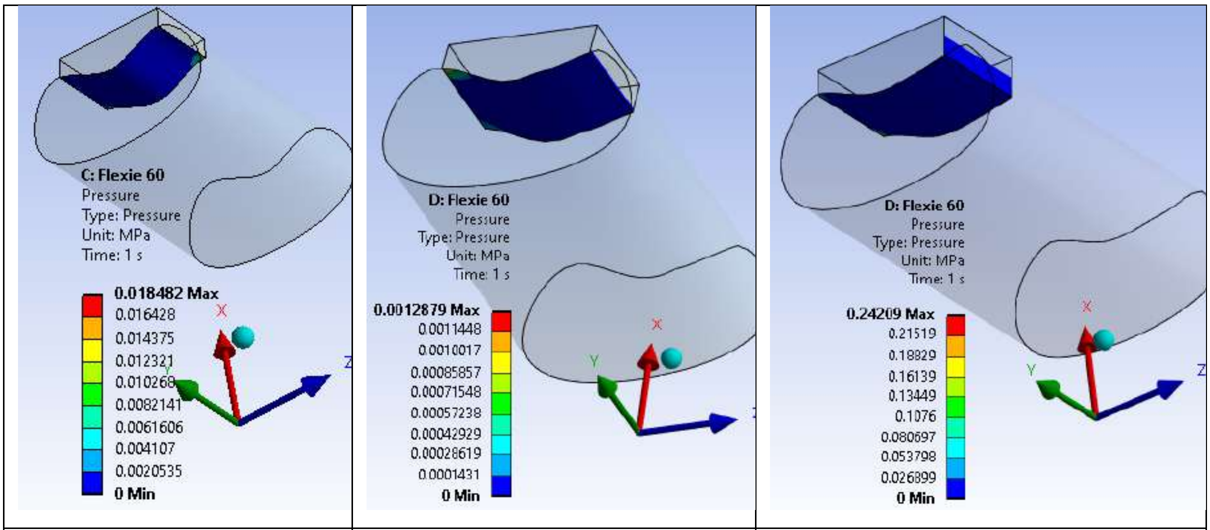

Case A-1	Case A-2	Case A-3

Fig. 21 Stress variation in the contact area - Flexion 60º

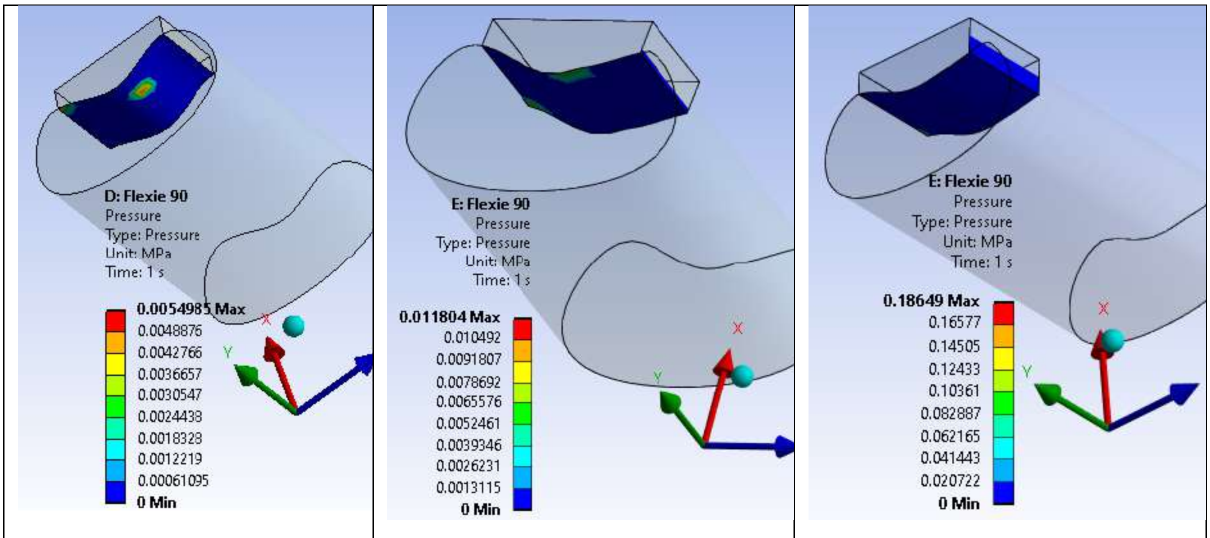

Case A-1	Case A-2	Case A-3

Fig. 22 Stress variation in the contact area - Flexion 90º

Fig. 23 shows the variation of the frictional stress that forms in the contact area.

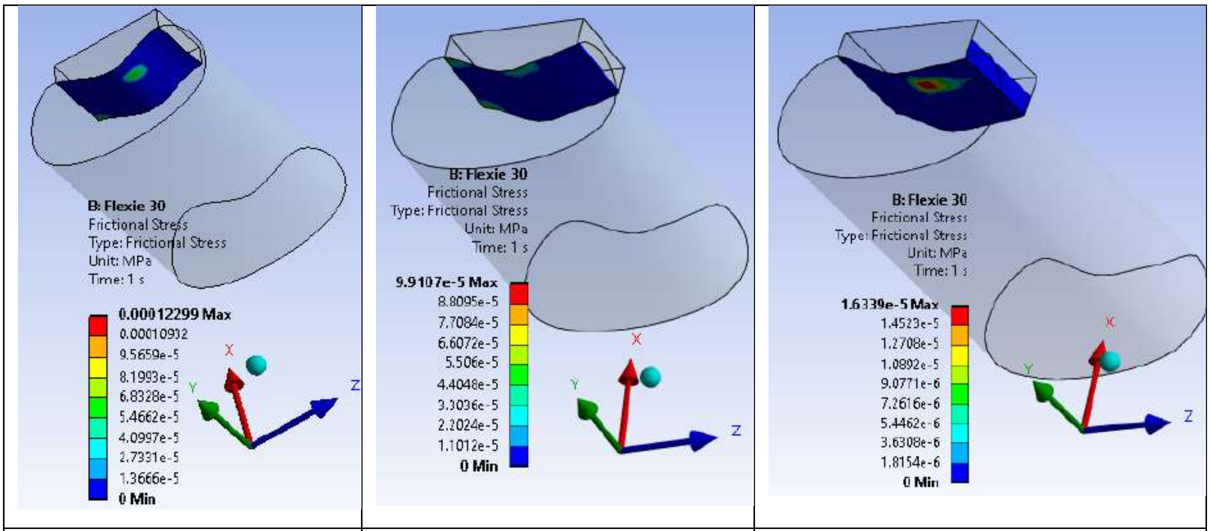

Case A-1	Case A-2	Case A-3

Fig. 23 Frictional stress variation in the contact area - Flexion 30º

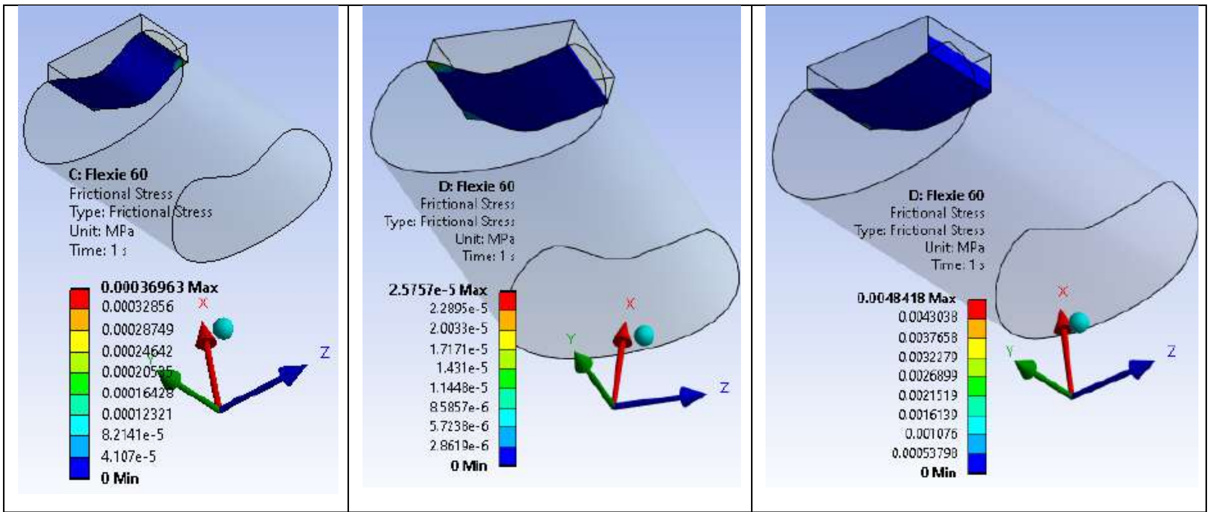

Case A-1	Case A-2	Case A-3

Fig. 24 Frictional stress variation in the contact area - Flexion 60º

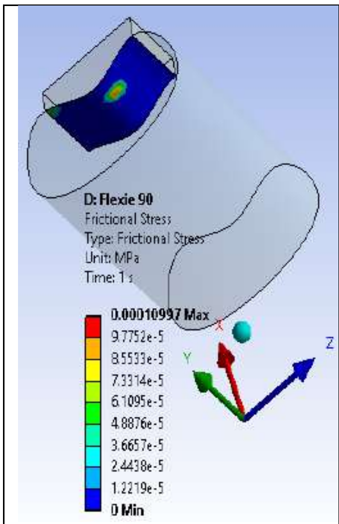	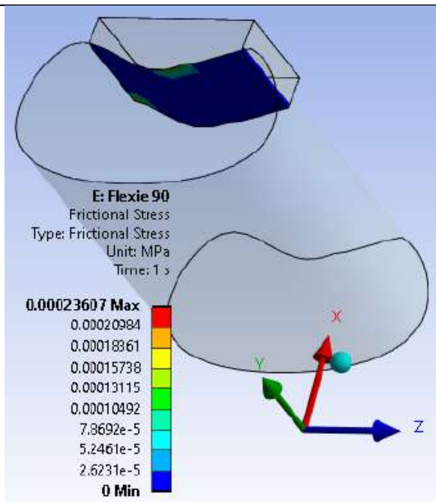	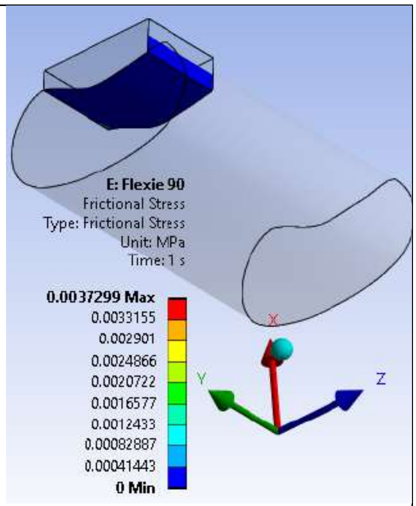
Case A-1	Case A-2	Case A-3

Fig. 25 Frictional stress variation in the contact area - Flexion 90^o

The analysis of frictional stress revealed lower values in the case of A3 compared to A1 and A2 in all 3 flexion situations, which denoted that the lower lateral trochlear inclination angle resulted in a frictional stress distributed over a larger area.

2. ***Case B-1, 2 and 3*** *- the patellofemoral joint system deviated from the biomechanical axis*

Following the numerical simulation performed, using the finite element method, the results obtained for the second case analyzed, in which a model that represented a situation often encountered in orthopedic practice was created, were analyzed by comparison with the results obtained for **Case A**, thus highlighting the phenomena that appeared in the contact area of the patellofemoral joint system in the situation in which the knee extensor mechanism assembly was deviated from the normal axis - biomechanical axis.

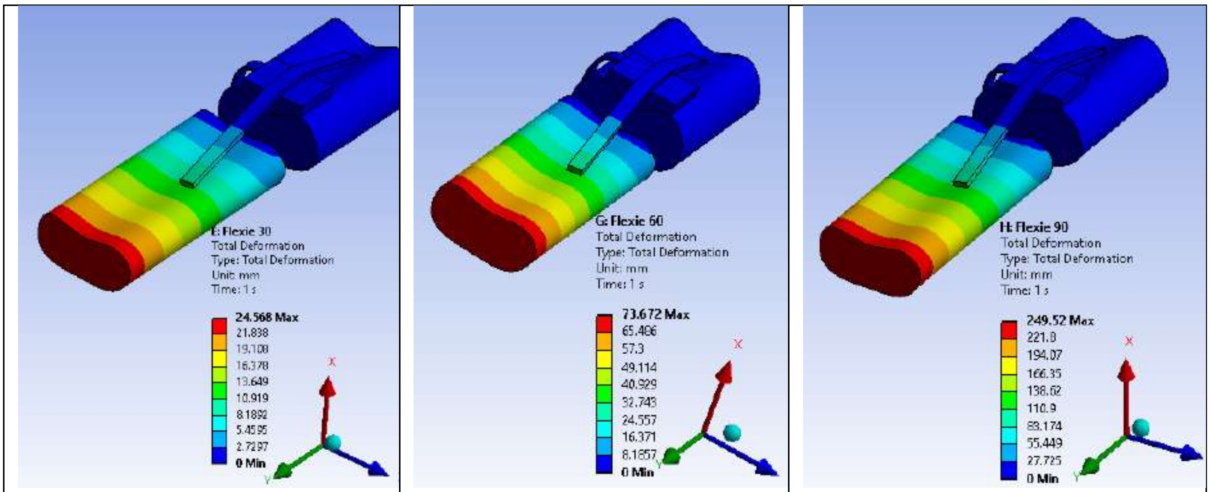

Flexion 30º	Flexion 60º	Flexion 90º

Fig. 26 Variation of the equivalent displacement in the model

The values presented in fig. 26 are approximately identical to the displacement value applied according to the flexion angle (Table 3).

Fig. 27-29 shows the distribution of the equivalent stress in the assembly, determined according to the von Mises criterion.

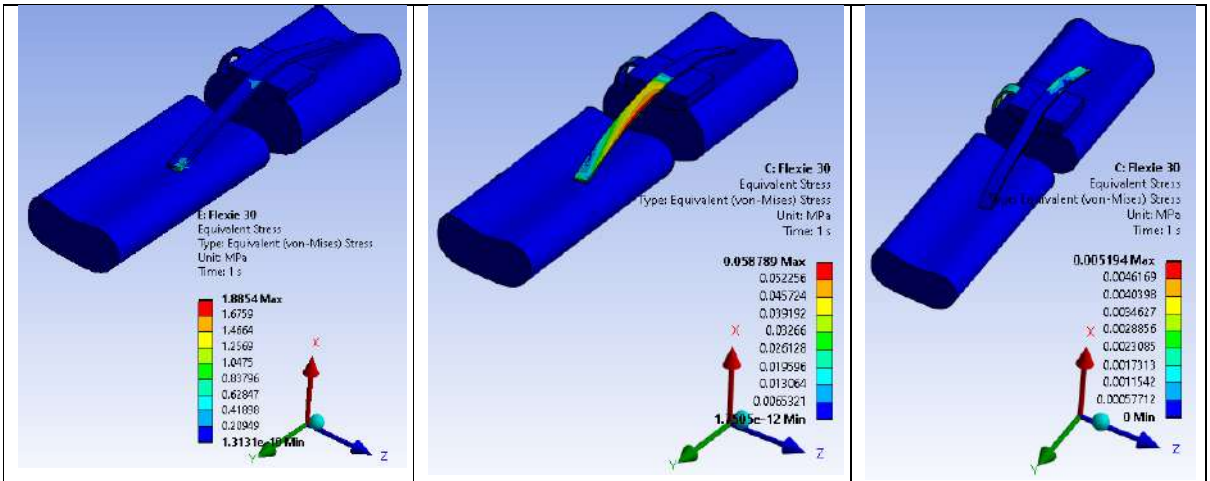

Case B-1	Case B-2	Case B-3

Fig. 27 Variation of the equivalent stress in the model - Flexion 30º

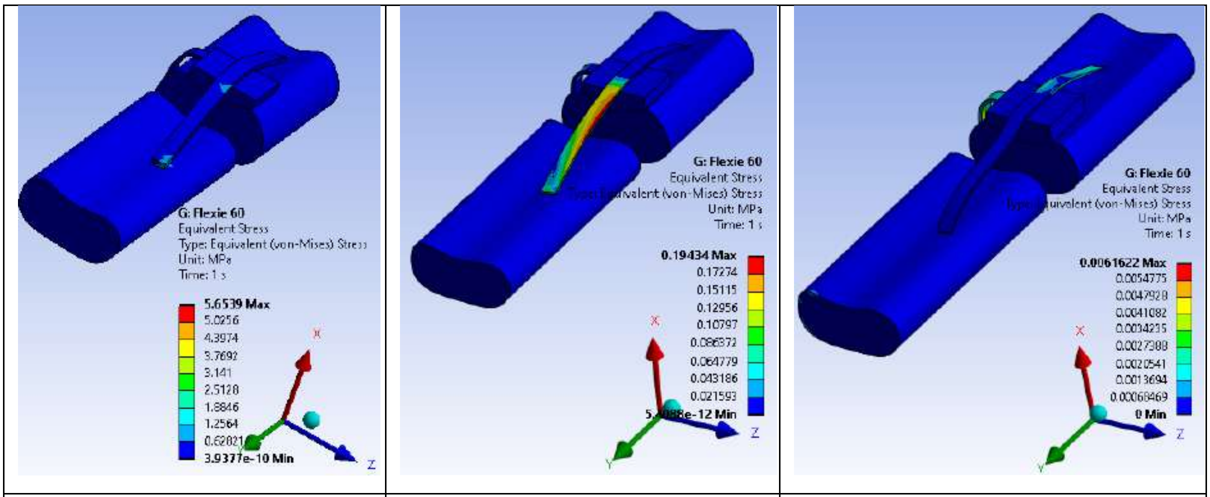

Case B-1	Case B-2	Case B-3

Fig. 28 Variation of the equivalent stress in the model - Flexion 60º

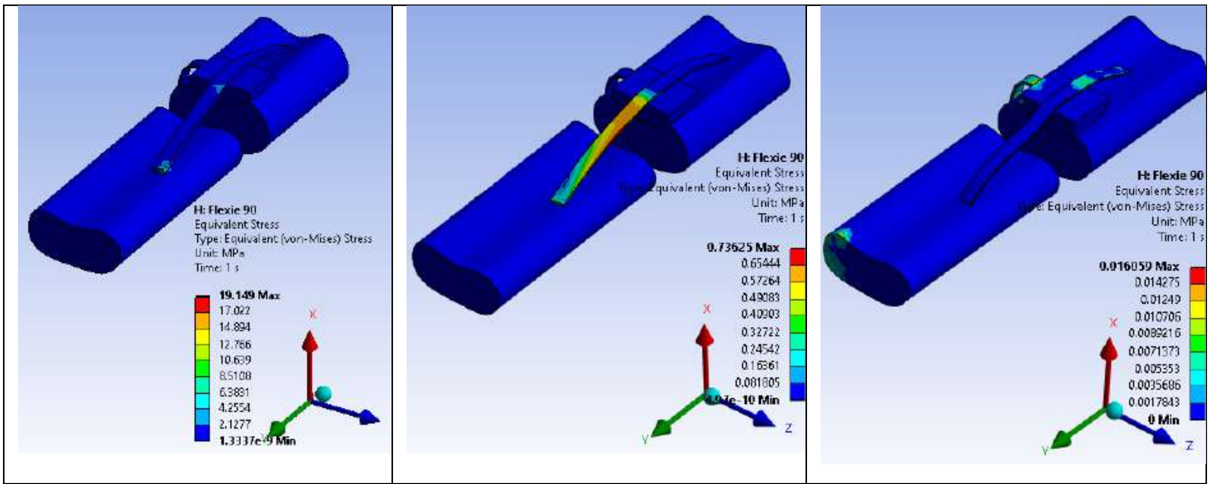

Case B-1	Case B-2	Case B-3

Fig. 29 Variation of the equivalent stress in the model - Flexion 90º

Analyzing fig. 27-29 it was noted that, for case B-1, the stress was concentrated around the connection of the ligament on the tibial component, the values of the equivalent stress increasing with the increase of the flexion angle. For case B-2, a smaller variation of the equivalent stress recorded on the connecting ligament of the components of the patellofemoral-tibial joint system was observed, and for case B-3, the stress decreased, concentrating in the medial ligament, this occurring as a result of the appearance of the sliding phenomenon between the patella and the femoral trochlear canal, due to the fact that the patella tends to come out of the joint system, exerting pressure on the medial patellofemoral complex represented in the MPFL simulation.

Fig. 30-32 present the movement of the connected components.

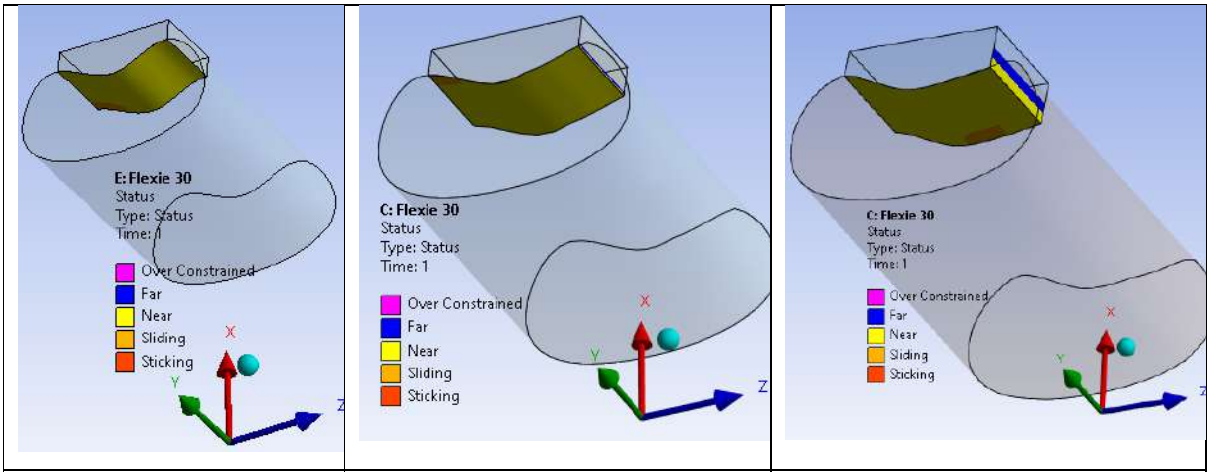

Case B-1	Case B-2	Case B-3

Fig. 30 Control elements in the patellofemoral contact area - Flexion 30º

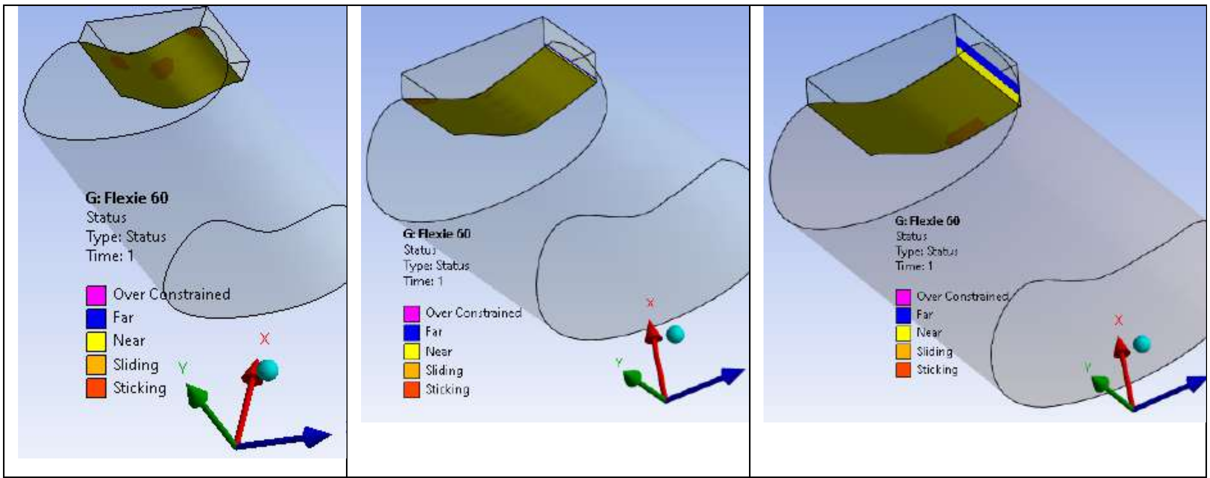

Case B-1	Case B-2	Case B-3

Fig. 31 Control elements in the patellofemoral contact area - Flexion 60º

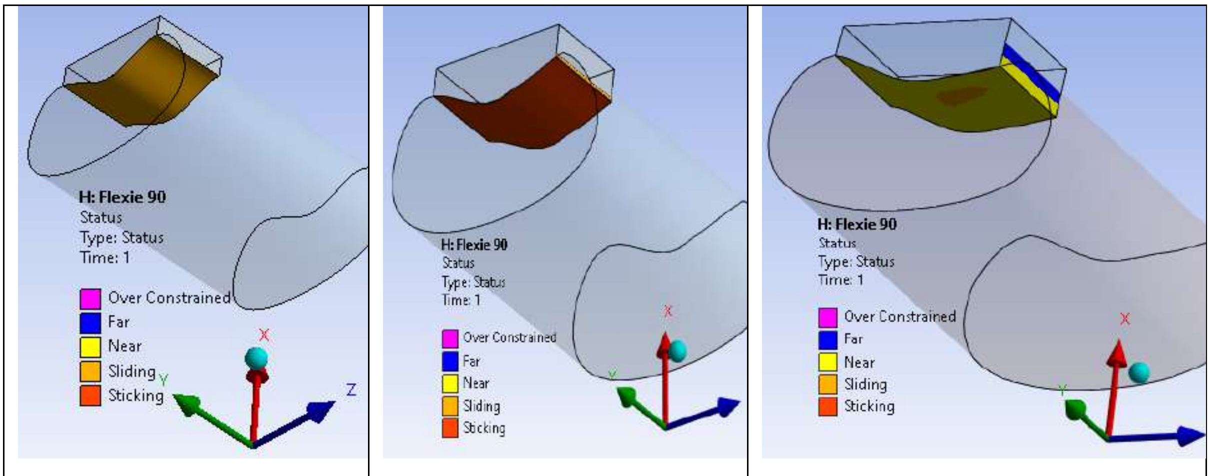

Case B-1	Case B-2	Case B-3

Fig. 32 Control elements in the patellofemoral contact area - Flexion 90º

Analyzing fig. 30-32 it was found that in cases B-2 and B-3, in certain areas (the most intensely colored), there was a malalignment of the contact surfaces between the patella and the femur, which led to the disconnection of the patellofemoral joint system. The most eloquent situation was represented by case B3, in which the applied pressure was correlated with the phenomenon of deplaning and lateral decoupling, a case related to the clinical situation of patellar dislocation.

Fig. 33-35 show the stress variation at the interface between the two connected components.

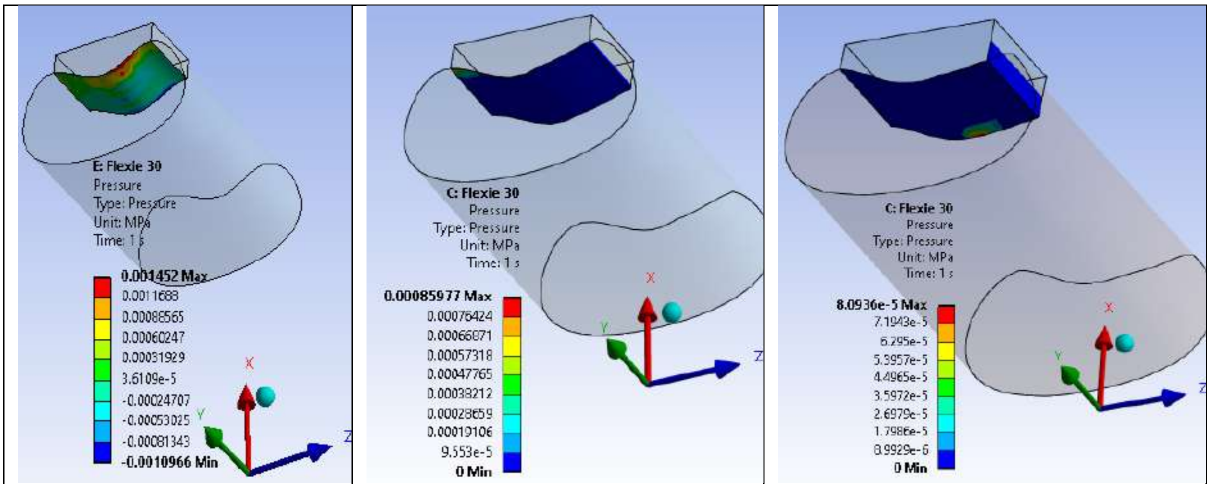

Case B-1	Case B-2	Case B-3

Fig. 33 Stress variation in the contact area - Flexion 30º

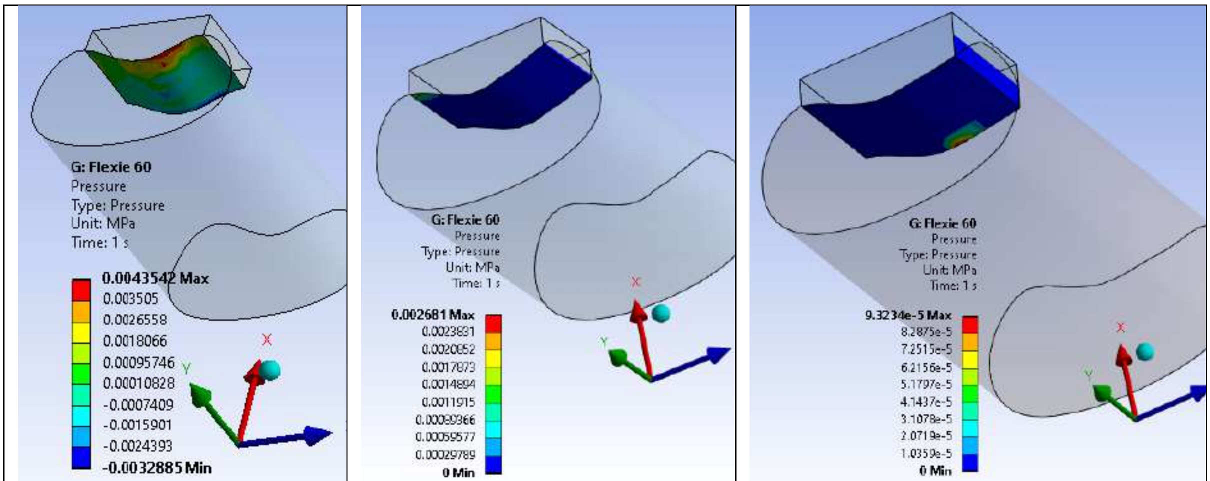

Case B-1	Case B-2	Case B-3

Fig. 34 Stress variation in the contact area - Flexion 60º

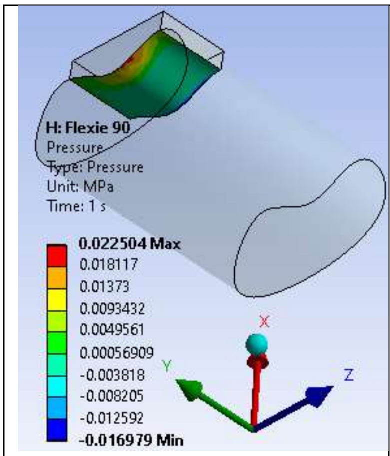

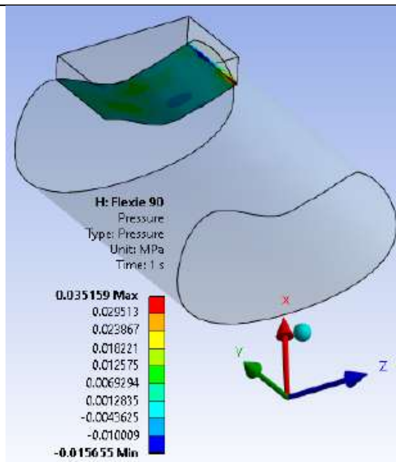

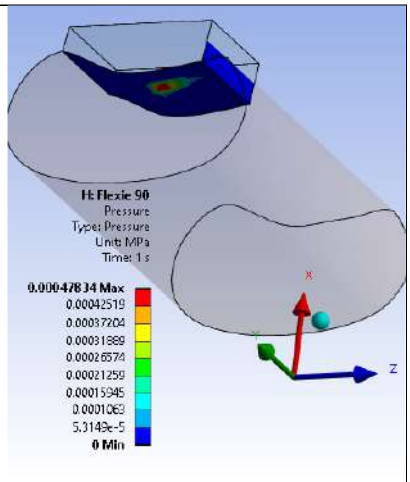

Case B-1	Case B-2	Case B-3

Fig. 35 Stress variation in the contact area - Flexion 90º

According to fig. 33-35, the effect of irregular stressing of the patellofemoral joint system was observed because the joint system was eccentric to the biomechanical axis. For these reasons, the stress values at the contact interface between the functional elements of the patellofemoral joint system decreased regarding value for the three cases. Therefore, an extensor mechanism system malaligned from the biomechanical axis was correlated with the situation of the successive decrease in the degree of lateral trochlear inclination with an inversely proportional decrease in the stress in the contact area.

Fig. 36-38 show the pressure variation resulting from friction at the interface between the contact surfaces of the two constituent components of the patellofemoral joint system.

Analyzing the evolution of the stress variation, it was observed that the values in the contact area for cases B-2 and B-3 decreased towards zero, which denoted the fact that the two components were no longer in contact, leading to the loss of stable balance of the patellofemoral joint system.

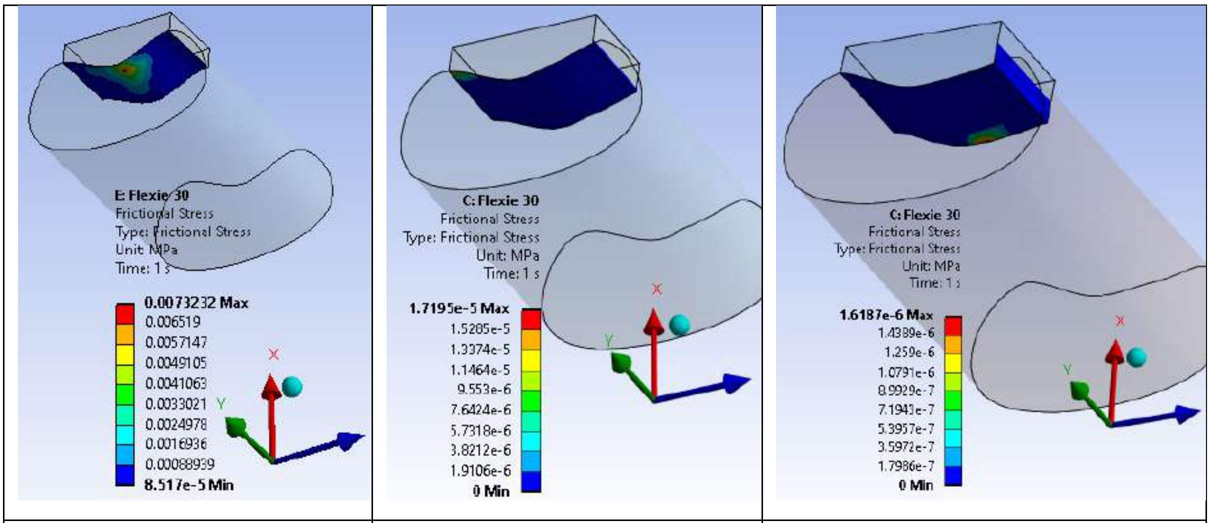

Case B-1	Case B-2	Case B-3

Fig. 36 Frictional stress variation in the contact area - 30º flexion

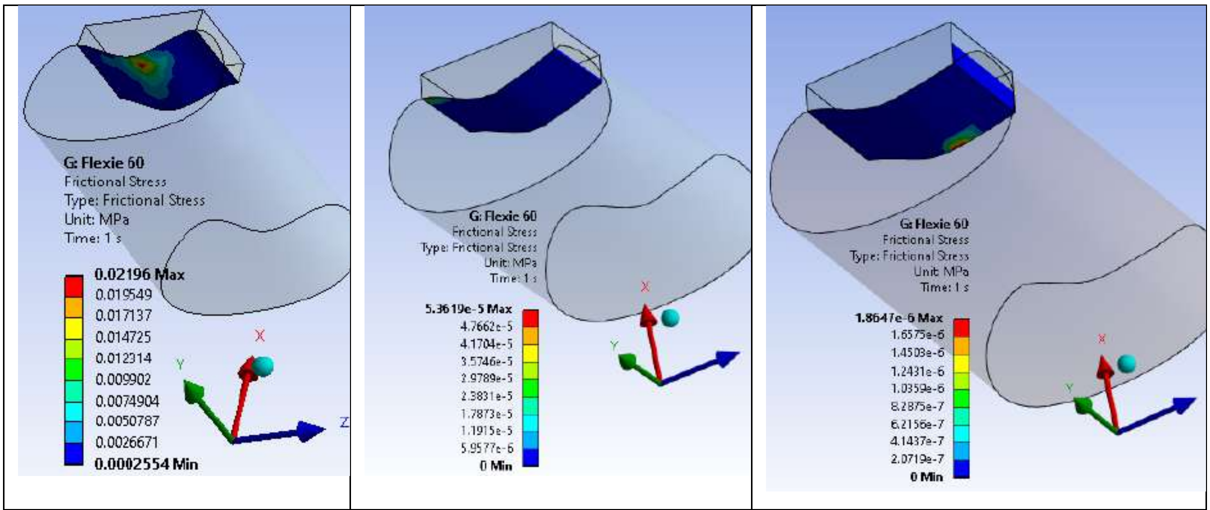

Case B-1	Case B-2	Case B-3

Fig. 37 Frictional stress variation in the contact area - Flexion 60º

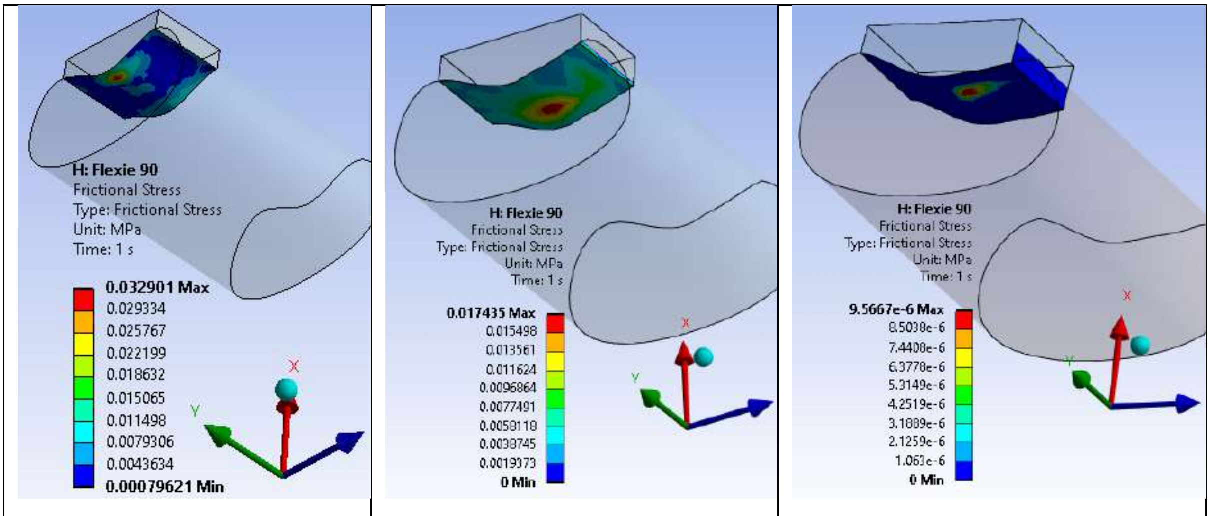

Case B-1	Case B-2	Case B-3

Fig. 38 Frictional stress variation in the contact area - Flexion 90º

3.3 Discussions

The analyzed model represents a parametric three-dimensional reproduction of the patellofemoral joint, which tried to represent the kinematics of the human patellofemoral joint in the situation of anatomical normality, but also to identify the biomechanical changes and consequences that occur in various pathological situations represented by the lateralization of the tibial tubercle correlated with the presence or the absence of a degree of trochlear dysplasia. Pressure changes, contact surface stresses, assembly stabilities and kinematic behavior over the entire plane of the knee flexion movement were searched and identified.

3.4. Conclusions

The finite element method represents a modern and current viable solution, which can be used with the aim of better knowing the kinetics and the changes that occur in the patellofemoral joint, both in the case of a normal anatomy and in situations of modified joint geometry. The current concepts of tibial tubercle osteotomy use the TT-TG distance with variation over 2 cm as the “gold standard”, representing a clear indication for surgery. However, the in-depth mathematical analysis reveals the situation in which the presence of a trochlear dysplasia, with a lateral trochlear inclination angle with low values, below the value of 8 degrees, causes a great danger of instability of the extensor mechanism, with the risk of patellar dislocation [20].

4. Designing an adjustable device for guiding tibial tubercle osteotomies in the case of patients with malalignment of the knee extensor mechanism

4.1 Introduction

The lower incidence of patellofemoral instability, compared to other orthopedic pathologies among the general population, has led to a relatively low interest of orthopedic surgeons in osteotomies of alignment of the extensor mechanism, the guiding devices for these osteotomies being extremely limited on the market today [21].

The aim of this study was to design a device to guide osteotomies at the level of the tibial tubercle in cases of lateralization. The premises, that the development of this device was based on, were the desire to improve surgical results by limiting possible complications, performing bone cutting sections as precise as possible and the capacity for increased reproducibility.

4.2 Design of the device

The osteotomy guiding device has many structural elements in its design, but it is based on three main elements that will be used in the surgical technique:

- the adjustable element for establishing the optimal position of the cutting block;
- the guiding element of the cutting blade and support for the mobile element for marking the exit path of the cutting blade;
- the movable and adjustable element for marking and establishing the output contour of the cutting blade.

4.3 The medical purpose of the guiding device for tibial tubercle osteotomies

The clinical aim of using such a device was based on the following aspects [22]:

1. Ease of use by any orthopedic surgeon with minimal training on how to use the guiding device.
2. Ensuring increased precision by guiding the cutting blade for osteotomy.
3. The possibility of tracking the output contour of the cutting blade using the mobile device.
4. Reduction of complications related to the free-hand osteotomies currently performed - intraoperative fractures.
5. Reduction of complications related to injury to soft parts during osteotomy.
6. Reduction of operative time and postoperative complication rates.
7. Versatility by adapting to the various possible anatomical variants.
8. Extended use and modularity through the possibility of osteotomy angle adjustment for all types of tibial tubercle osteotomies in extensor mechanism dislocations.
9. Reduced costs due to the material that allows resterilization, reuse and increased endurance of the assembly components.
10. Improving postoperative functional recovery and promoting faster and lower-risk consolidation.

4.4 Properties of the medical guiding device intended for use in tibial tubercle osteotomies for malalignment of the knee extensor mechanism

The design was carried out using SolidWorks 3D CAD software version 2021 SP2.0, which is a very stable reference program that performs computer-aided modeling and design (CAD) and computer-aided engineering (CAE) [22].

The device was designed from a material with characteristics of endurance, hardness, corrosion resistance and low production cost. DIN EN 1.4401 (X5CrNiMo17-12-2) material, from which the guiding device was designed, is based on austenitic stainless steel with molybdenum content. The chemical properties of molybdenum give the material a higher corrosion resistance compared to 1.4301(X5CrNi18-10), when mainly used in environments with a high content of chlorides and non-oxidizing acids, such as the solutions used in the medical washing and sterilization process [23].

4.5 Constituent elements of the guiding device

The following assemblies represent the constituent elements of the guidance device:

1. Guide pin - its role is to establish the position of the guide pin inserted anteroposteriorly to the proximal tibia. Its shape was conceived and designed to guide the two axes, longitudinal and transversal, of the tibia. In this situation, the technique involves the introduction of the guide pin and the use of the "free-hand" technique, but the use of the guide pin is preferred.
2. Adjustable cutting guide device - this assembly includes three adjustable gears to tailor the necessary modifications. The optimal position of the cutting guide block can be adjusted, as well as the inclination angle of the desired future osteotomy. It allows the use of the inclination angle with preset values of 45°, 60°, 90°, but it is also possible to opt for variations between these angles, leaving the degree of inclination of the osteotomy tranche to be determined by the surgeon.
3. The cutting blade guide device is designed to be attached to the bony structure of the tibia, to which it will be fixed with two pins inserted through special slots. The design of the cutting guide block will allow it to be attached to the adjustable cutting guide device by a special bolt, thus facilitating the optimal position to perform the desired osteotomy. The design of the specimen allows the mobilization in the superior and inferior planes for an ideal positioning. The anterior osteotomy slot serves as a pocket for the cutting marker that will help design the osteotomy path on the opposite side of the tibial cortex.

4. The connecting element between the cutting blade guide device (component 3) and the adjustable cutting guide device (component 2) is the cutting guide bolt. It will be fixed to component 3 by screwing and will be locked in the final position on component 2 by the locking screw.
5. The cutting blade exit marking device - the functional role of this structure is to make the projection of the future osteotomy tranche at the contralateral cortex. Following the future contour can guide the orthopedic surgeon in the correct positioning of the cutting guide block and the need for possible corrections to be made.
6. The auxiliary assemblies are represented by the spacer spatula with the role of protecting the soft structures at the exit point of the cutting blade and forceps to extract the guide pins used to fix the osteotomy blocks.

4.6 Discussions

The osteotomy of the tibial tubercle represents a surgical intervention with an increased degree of complexity, presenting a considerable amount of possible complications. Some of the possible major complications are mentioned, namely non-consolidation in the osteotomy area or the risk of fracture. A possible cause for these complications is the application of osteotomy surgical techniques without the use of guiding aids. The extensive use of these guide assemblies would considerably decrease the incidence of complications [24,25].

4.7 Conclusions

The assembly described in the conducted study has the role of supporting orthopedic surgeons to increase the efficiency of the operation by increasing the precision of the osteotomies of the tibial tubercle. The use of guiding devices does not change the surgical technique, the surgeon applying the classical intraoperative steps.

Osteotomy of the tibial tubercle remains an undisputed surgical landmark in the treatment of patients with patellar instabilities and significant malalignment of the extensor mechanism. The introduction of guidance devices during the surgery would bring a projection of the osteotomy tranches made many times with a subjective foundation. The guiding devices would guarantee a better protection of the soft parts during the surgery, an objectification of the surgical gestures with the improvement of the functional results and the decrease of long-term complications [26,27].

5. Study on the usefulness of the tibial tubercle distance - posterior intercondylar arch as a new measurement in the diagnosis and surgical treatment by tibial tubercle osteotomy in patients with knee extensor mechanism malalignment

5.1 Introduction

Tibial tubercle osteotomy is a frequently used procedure to correct pathological patellar tracking. The indication for osteotomy is currently based on the tibial tubercle-trochlear groove (TT-TG) distance with a value over 20 mm, the effectiveness and validity of this parameter, proposed by Dejour in 1994, being proven by numerous studies [28]. However, in patients with trochlear dysplasia, the TT-TG distance is less reproducible, especially in patients with high grade dysplasia. TT-TG values determined on CT are not always equal to those measured on MRI, with an average difference between 2.2 and 4.16 mm, according to literature data [29].

The aim of this study was to determine the correlations between a new parameter, namely the tibial tubercle-posterior intercondylar arch distance (TT-IC), with the TT-TG distance, but also with other extensor mechanism malalignment parameters that associate trochlear dysplasia, lateral trochlear slope, trochlear angle and trochlear facet asymmetry and to establish a possible indication for osteotomy in these patients.

5.2 Materials and methods

In the current study, the data of 60 patients, diagnosed with extensor mechanism malalignment, who benefited from osteotomy surgery, during the period 2016-2022, were analyzed. Patients from the Orthopedics and Traumatology Clinic of the Bucharest University Emergency Hospital were included in the study, obtaining the prior approval of the hospital’s Ethics Commission, the patients’ informed consent to be included in the study group and respecting international norms regarding the ethics and deontology of scientific research. The patients were evaluated by performing a CT and MRI of the operated limb and the known diagnostic parameters, such as the TT-TG distance, the trochlear angle, the trochlear lateral slope or the trochlear asymmetry, but also the TT-IC parameter, were determined.

The statistical analysis was performed using the IBM SPSS Statistics version 21 program. The statistical tests used in the analysis were: the **Mann-Whitney U test**, the **Wilcoxon test** and the **Chi-Square test**, for the association between numerical variables, as well as the **Phi correlation coefficient** for determining correlations between these variables. The value of statistical significance was considered $p<0.05$.

5.3 Results

The mean age of the patients was 25.57 years (standard deviation 5.013; CI: [24.27, 26.86]), without major gender differences, with a predominantly female distribution of cases, i.e. 80% were women (n=48), and 20% men (n=12).

5.4 Evaluation of lateral trochlear inclination and association with TT-IC on CT

Significant differences between the TT-TG and TT-IC distances were also highlighted in the case of patients with **trochlear lateral slope > 11 (n=42)**, the TT-IC values also being much higher than those of the TT-TG **(mean values 2.42 vs. 2.01) (Z = –5.691, p<0.001)**.

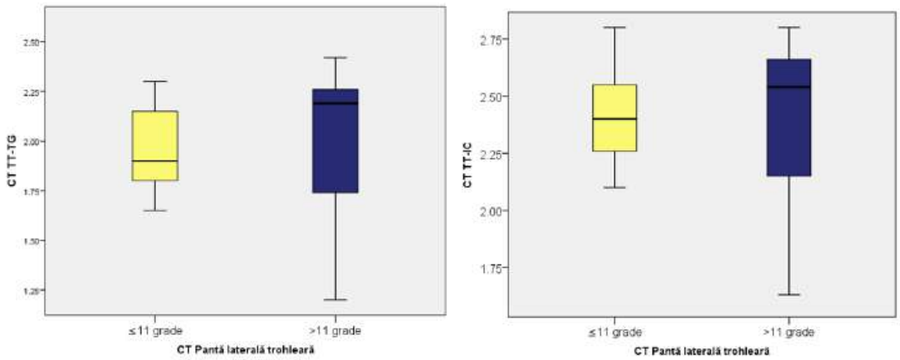

Graphs 15,16. Distribution of cases according to TT-TG, respectively TT-IC in patients with trochlear lateral slope < 11 degrees, respectively > 11 degrees

5.5 Evaluation of trochlear facet asymmetry of the trochlear facets and association with TT-TG, respectively TT-IC on MRI

Regarding **trochlear facet asymmetry**, patients who presented trochlear facet asymmetry (measured on MRI) had TT-TG values between 1.74 and 2.30, with a mean value of 1.9867 (standard deviation 0.20, CI: [1.89; 2.07]) and a median value of 1.90. (n=21), while patients **without trochlear facet asymmetry** had TT-TG values between 1.20 and 2.42, with a mean value of 1.9886 (standard deviation 0.37, CI: [1.84, 2.13]) and a median of 2.2 (n=29). The TT-TG distance did not show statistically significant differences between patients with trochlear facet asymmetry and patients without asymmetry (p=0.510).

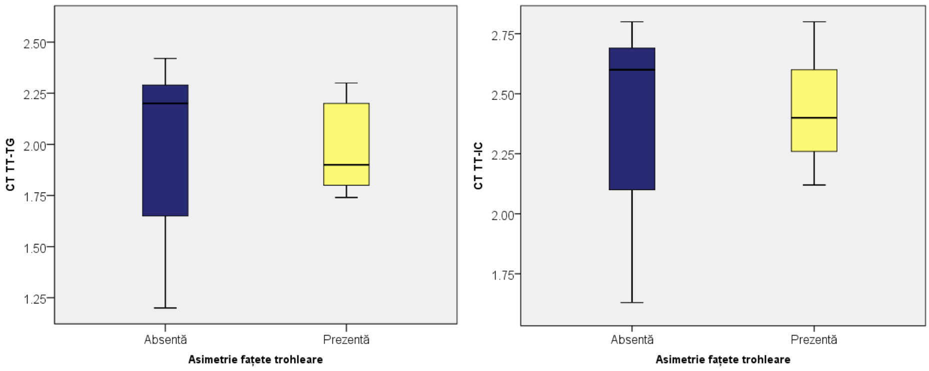

Graphs 17,18. Distribution of cases according to TT-TG, respectively TT-IC in patients with and without trochlear facet asymmetry

5.6 Evaluation of trochlear angle and association with TT-TG, respectively TT-IC on CT and MRI

Patients with a **trochlear angle ≤ 140 degrees** (measured on MRI) had TT-TG values between 1.20 and 2.42, with a mean value of 2.02 (standard deviation 0.36, CI: [1.87, 2.16]) and a median value of 2.24 (n=27), while patients with a **trochlear angle above 140** had TT-TG values between 1.43 and 2.30, with a mean value of 1.94 (standard deviation 0.23, CI: [1.84, 2.04]) and a median of 1.90 (n=23). The TT-TG distance did not show statistically significant differences between patients with trochlear angle ≤ 140 and those with trochlear angle over 140 degrees (p=0.149).

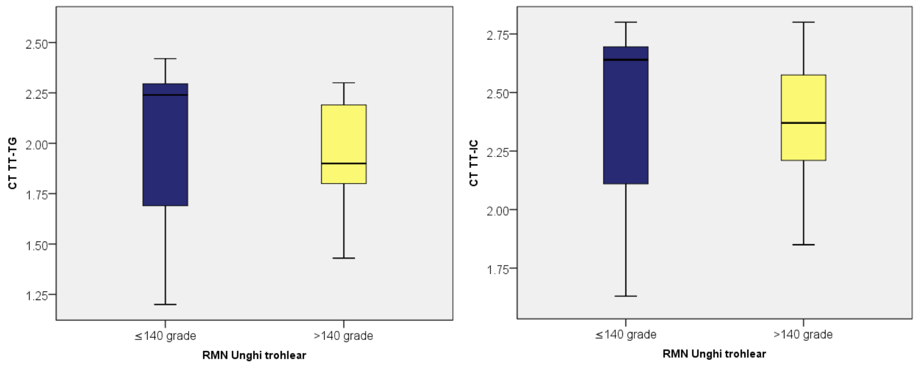

Graphs 19,20. Distribution of cases according to TT-TG, respectively TT-IC and the association with the trochlear angle determined on MRI

Regarding the evaluation on CT, in the group of patients who had a **trochlear angle ≤ 140 degrees** (measured on CT), the TT-TG values were between 1.20 and 2.42, with a mean value of 2.04 (standard deviation 0.33, CI : [1.92; 2.16]) and a median value of 2.20 (n=33), while in those with a **trochlear angle above 140**, the TT-TG values were between 1.43 and

2.30, with a mean value of 1.94 (standard deviation standard 0.23, CI: [1.85, 2.03]) and a median value of 1.90 (n=26). The TT-TG distance did not show statistically significant differences between patients with trochlear angle ≤ 140 and those with trochlear angle over 140 degrees (p=0.056).

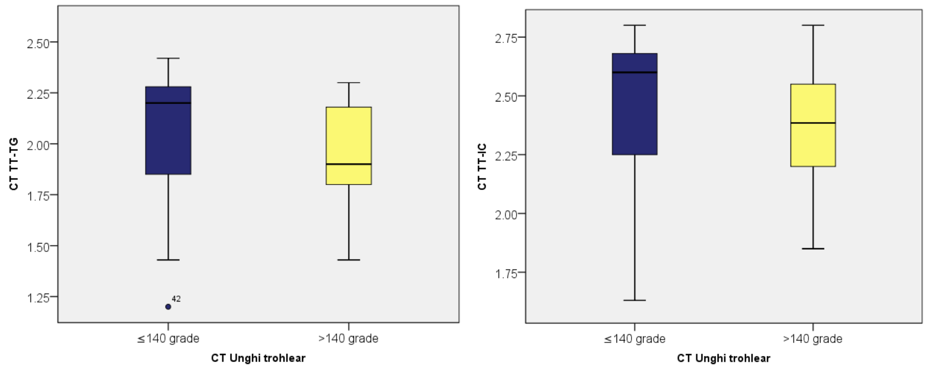

Graphs 21,22. Distribution of cases according to TT-TG, respectively TT-IC and the association with the trochlear angle determined by CT

5.7 Evaluation of TT-TG and TT-IC parameters by ROC curves

Both the TT-TG distance and the TT-IC distance showed reduced specificity and sensitivity regarding the predictability of patients with **trochlear lateral slope < =11 degrees** (in the case of TT-TG AUC 0.411, cut-off value 1.86 cm, sensitivity 56 %, specificity 36%, respectively in the case of TT-IC AUC 0.490, cut-off value 2.25 cm, sensitivity 75%, specificity 36%, p=0.313, respectively 0.91).

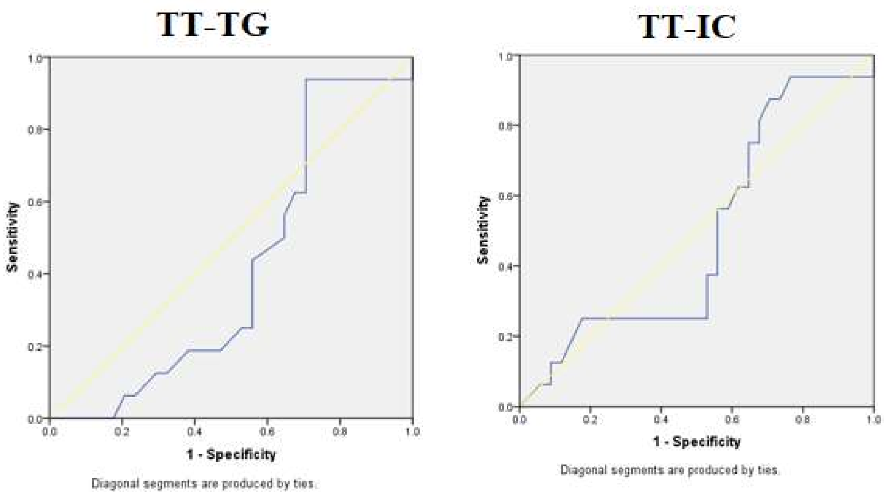

Graphs 23,24. ROC curves for the TT-TG and TT-IC distance in patients with trochlear lateral slope < 11 degrees

By analyzing the ROC curves in patients with Elmslie-Trillat medialization osteotomy, both the TT-TG parameter and the TT-IC parameter had high sensitivity and specificity, statistically significant, with higher values for the TT-IC distance being predictive for this type of surgical intervention (in the case of TT-TG AUC 0.778, cut-off value 1.86 cm, sensitivity 78%, specificity 62%, p=0.001, respectively in the case of TT-IC AUC 0.787, cut-off value 2.25 cm, sensitivity 85 %, specificity 62%, $p<0.0001$).

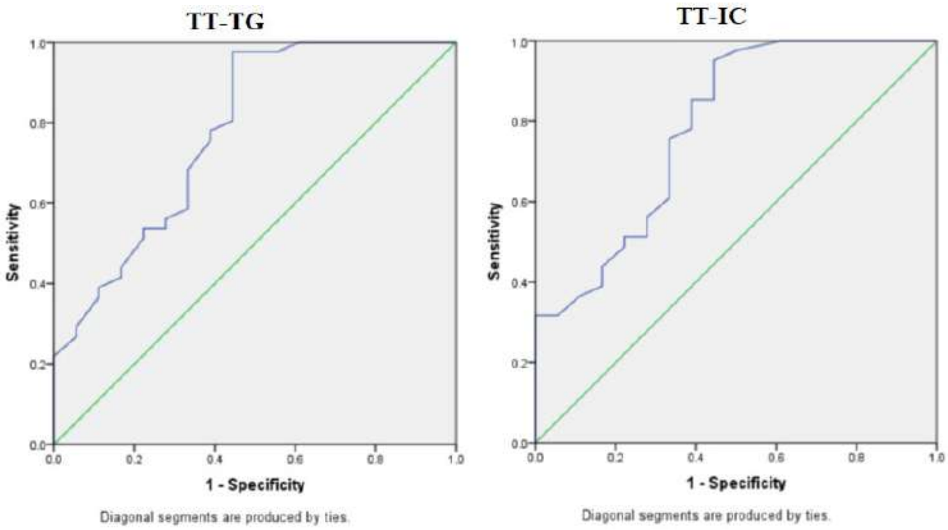

Graphs 25,26. ROC curves for the TT-TG and TT-IC distance in patients with Elmslie-Trillat osteotomy

5.8 Discussions

Successive studies have established that the increased value of the TT-TG distance is a predictive indicator for the presence of patellar instabilities, and the value over 20 mm represents the gold standard regarding the formal indication to perform the medialization osteotomy of the tibial tubercle [30]. However, this axial measurement presented limitations due to low reproducibility, especially in patients with trochlear dysplasias, especially in patients with advanced trochlear dysplasias with a trochlear angle and values close to 180 degrees - flat trochlea. This situation arose from the difficulty to accurately measure and establish the deepest point of the trochlear groove [31-33]. Thus, a new landmark was needed, which could be used and have a greater efficiency in establishing the lateralization of the tibial tubercle in patients with advanced trochlear dysplasia.

5.9 Conclusions

The study created the premises for a new axial measurement that quantifies the degree of lateralization of the tibial tubercle in patients with patellar instability. Following the analysis, higher values of the new landmark TT-IC compared to TT-TG were found in the whole group of patients, but the values were clearly higher in patients with trochlear dysplasia. Therefore, in the case of the analysis of a patient with patellar instability and trochlear dysplasia, it is necessary to consider the TT-IC value, in addition to the classic landmark represented by the TT-TG distance, to correctly quantify the indication for osteotomy of the tibial tubercle.

Personal contributions

The first chapter of the special part represents a study that evaluates the influence of the indices obtained from the axial measurements made by computer tomography, magnetic resonance and conventional radiographs. Indicators such as TT-TG distance, trochlear angle, patellofemoral tilt angle, lateral trochlear inclination angle, convergence angle, patellar tip, patellar height with Insall-Salvati indicators, Caton-Deschamp index, Blackbourne-Peel index, trochlear facet asymmetry, correlation of pre- and postoperative Kujala, Lysholm and Tegner functional scales with variables such as BMI, age or type of intervention performed, were measured.

The analysis of the group of patients who underwent surgery highlights that a complete and thorough analysis by axial imaging is extremely important, to establish all the anatomical and biomechanical causes that lead to the appearance of the phenomenon of patellofemoral instability, pain, or finally, excessive cartilage wear with the appearance of medial compartment ostheoarthritis.

The next chapter represents a three-dimensional parametric reproduction of the patellofemoral joint using the finite element method, which tried to identify the kinematics of the joint both in the case of a normal biomechanical axis and in the case of a biomechanical malalignment by lateralizing the position of the tibial tubercle. Additionally, dynamic simulations for values of 30, 60 and 90 degrees of knee flexion were introduced in the analysis and various lateral trochlear inclination angles appeared.

A degree of trochlear dysplasia quantified by the low lateral trochlear angle was identified in the case of a malalignment of the extensor mechanism by lateralizing the tibial tubercle, which led to a more extensive contact surface, with lower stress. Thus, cartilage wear was reduced in this situation, but the degree of instability of the entire complex increased.

By using a computer-aided modeling software, SolidWorks 3D Cat, a device was designed to be used in the case of tibial tubercle osteotomy. The design and planning were done extremely elaborately, with technical design and execution plans for each structural component of the device, being able to move on to its execution. The material used, represented by austenitic steel with a high content of molybdenum, is resistant to corrosion, can withstand medical resterilization and, thus maintains a low cost of manufacturing and maintenance of the device.

By using the device in the surgical technique, the efficiency will escalate by increasing the precision of the osteotomy, thus boosting the interoperative reproducibility. The design and development of the device was versatile, thus being able to be used for various osteotomy surgical techniques by changing the angle of inclination of the osteotomy, and being able to simulate the exit point of the cutting blade on the contralateral cortex with the aid of the osteotomy verification guide.

The following chapter highlighted the perspective of using new measurements to quantify the lateralization of the tibial tubercle in patients with trochlear dysplasia. The classic TT-TG distance measurement system presented limitations such as the impossibility of accurately identifying the deepest point within the trochlear groove (TG), thus bringing flawed values into the diagnostic and treatment algorithm. The new landmark considers the tangent to the posterior intercondylar arch (IC) as the bony landmark for the new measurement, demonstrating better fidelity for identifying the lateralization of the tibial tubercle.

The study compared the two types of measurements, both TT-TG and TT-IC, as being good indicators for the predictability of patellar instability, however, in the case of patients with trochlear dysplasia, TT-IC had a higher accuracy.

6. General conclusions

The first part of the PhD thesis highlighted the fundamental anatomical elements of the knee and the extensor mechanism for a thorough and complex understanding of the notions of biomechanics of the patellofemoral joint. The forms of patellar dysplasia and the forms of trochlear dysplasia were identified, together with their inclusion in the established classifications from literature.

Advanced notions of biomechanics of the extensor mechanism were exemplified, with the understanding of the patellofemoral posterior force vector, the patellofemoral joint reaction force, the identification of the distribution of contact areas and pressure expressed at the level of the femoral trochlea and the patella, depending on the degrees different from knee flexion.

The notions of biomechanics, such as the ratio between the force modulus of the quadriceps and the force modulus of the patellar tendon in extension, as well as the different changes in the flexion angle, were identified. The two nonlinear mathematical equations applicable to the patellofemoral joint in the two-dimensional analysis were reviewed, which help establishing the correlations between different parameters, such as the angle of inclination of the flexion, the length of the patellar tendon, the position of the patella tangent to the trochlear canal.

Also, the clinical and imaging diagnostic methods were identified with an emphasis on the measurement parameters made by computed tomography and nuclear magnetic resonance imaging with axial measurements, and the correlations between the indicators, the types of surgical interventions and the postoperative evaluation scales, were established.

At the end of the general part, the operative techniques used in current practice, in the case of extensor mechanism malalignments, were listed and described, specifying all the operative steps that must be taken.

At the beginning of the general part, the correlations of the imaging indicators performed with the patient's antecedents, variables such as age, sex, BMI, the type of intervention performed, the correlation with the functional evaluation scales and the rate of possible complications, were quantified. The results were predictable and many correlated with the notions and references already present in literature, but the problem of a more correct and complex evaluation of all the indicators and the identification of all the components arose, which led to the symptoms of patellar instability.

An elaborate analysis of the finite element modeling of the patellofemoral joint was then performed. Although the method presented indisputable advantages in terms of the results and predictions obtained, the subject related to the opportunity of application in current practice remained open, as the method is time, resources and computing technique consuming. Its validation must be performed most of the time on cadaveric models, and during the analysis it is necessary to introduce many parameters to accurately simulate the normal or pathological biomechanics of the joint.

The third research of the PhD study was based on the development and design of a device for guiding osteotomies, which would bring immeasurable benefits to the surgical technique. The modularity which it was designed with allows it to be adapted to all types of tibial osteotomies described and used to date, with the establishment and choice of the angle of inclination of the osteotomy and adaptation to the different anatomical morphotypes present in the general population. The osteotomy tracking device helps the surgeon objectify the future osteotomy, in case of a deficiency, the instrumentation allowing the adjustments to be repeated until a satisfactory result is obtained. The possibility of performing a guided osteotomy will increase accuracy and efficiency, decrease the complication rate and improve functional outcomes. The material from which it is designed ensures reliability and endurance, with low production and maintenance costs.

The final chapter of the PhD thesis, from the special part, highlighted the objectification of a new parameter for the establishment of the lateralization of the tibial tubercle, especially in the case of patients with high degrees of trochlear dysplasia. The results of the study presented the promising premises of a new TT-IC measurement, which can be used to complement the already established TT-TG distance, for a more correct and complete quantification of the extensor mechanism malalignment status. However, further research and studies are needed on larger groups of patients, considering multicenter studies, to obtain the most conclusive and statistically relevant results.

Therefore, it is necessary to understand the complexity and multifactorial character of the etiology of malalignments of the knee extensor mechanism. The optimization of the diagnostic and treatment algorithm must consider the multitude of associated risk factors, age, level of activity, and the choice of the individualized therapeutic option for each patient. The best functional results are obtained by the complete investigation, by using available imaging methods, the establishment of all parameters, and the choice of the optimal surgical treatment.

References

1. Dejour DH (2013) The patellofemoral joint and its historical roots: the Lyon School of Knee Surgery. Knee Surg Sports Traumatol Arthrosc 21(7):1482–1494.
2. Robert A. Duerr, Aakash Chauhan, MBA Darren A. Frank, Patrick J. DeMeo, Sam Akhavan, An Algorithm for Diagnosing and Treating Primary and Recurrent Patellar Instability, JBJS REVIEWS 2016;4(9):e2.
3. Alice J. S. Fox, Florian Wanivenhaus, Scott A. Rodeo, The Basic Science of the Patella: Structure, Composition, and Function, J Knee Surg 2012;25:127–142.
4. Jorge Chahla, Robert Smigielski, Robert F. LaPrade, John P. Fulkerson, An Updated Overview of the Anatomy and Function of the Proximal Medial Patellar Restraints

(Medial Patellofemoral Ligament and the Medial Quadriceps Tendon Femoral Ligament), Sports Med Arthrosc Rev Volume 27, Number 4, December 2019.
5. Freehafer AA. A study of the function of the patella. Clin Orthop Relat Res 1962;25:162–167.
6. Thijs Y, Van Tiggelen D, Roosen P, De Clercq D, Witvrouw E. A prospective study on gait-related intrinsic risk factors for patellofemoral pain. Clin J Sport Med. 2007; 17: 437-445.
7. Amis AA, Oguz C, Bull AM, Senavongse W, Dejour D. The effect of trochleoplasty on patellar stability and kinematics: a biomechanical study in vitro. J Bone Joint Surg Br. 2008; 90: 864-869.
8. Gerd Diederichs, Ahi S. Issever, Sven Scheffler, MR Imaging of Patellar Instability: Injury Patterns and Assessment of Risk Factors RadioGraphics 2010; 30:961–981.
9. Alexander Zimmerer, Christian Sobau and Peter Balcarek, Recent developments in evaluation and treatment of lateral patellar instability, Journal of Experimental Orthopaedics (2018) 5:3.
10. Damasena I, Blythe M, Wysocki D, et al. Medial patellofemoral ligament reconstruction combined with distal realignment for recurrent dislocations of the patella: 5-year results of a randomized controlled trial. Am J Sports Med. 2017;45:369–376.
11. Hetsroni I, Mann G, Dolev E, et al. Combined reconstruction of the medial patellofemoral and medial patellotibial ligaments: outcomes and prognostic factors. Knee Surg Sports Traumatol Arthrosc. 2018;27:507–515.
12. Steensen RN, Dopirak RM, Maurus PB (2005) A simple technique for reconstruction of the medial patellofemoral ligament using quadriceps tendon graft. Arthroscopy 21:365–370.
13. Fucentese SF, Schöttle PB, Pfirrmann CW, Romero J. CT changes after trochleoplasty for symptomatic trochlear dysplasia. Knee Surg Sports Traumatol Arthrosc 2007;15(2):168–174.
14. Schöttle PB, Fucentese SF, Pfirrmann C, Bereiter H, Romero J. Trochleaplasty for patellar instability due to trochlear dysplasia: a minimum 2-year clinical and radiological follow-up of 19 knees. Acta Orthop 2005;76(5):693–698.
15. Naveed MA, Ackroyd CE, Porteous AJ. Long-term (ten- to 15-year) outcome of arthroscopically assisted Elmslie-Trillat tibial tubercle osteotomy. Bone and Joint Journal 2013;95(B):478–85.

16. Tigchelaar S, Van Essen P, Bénard M, Koëter S, Wymenga A. A self-centring osteotomy of the tibial tubercle for patellar maltracking or instability: Results with tenyears' follow-up. Bone and Joint Journal 2015;97-B:329–36.
17. Kwak SD, Colman WW, Ateshian GA, Grelsamer RP, Henry JH, Mow VC. Anatomy of the human patellofemoral joint articular cartilage: surface curvature analysis. J Orthop Res 1997;15 (3):468–472.
18. Zhe Du, Shichang Chen, Mengning Yan, Bing Yue, You Wang, Differences between native and prosthetic knees in terms of cross-sectional morphology of the femoral trochlea: a study based on three-dimensional models and virtual total knee arthroplasty, BMC Musculoskeletal Disorders (2017) 18:166.
19. J. W. Fernandez, P. J. Hunter, An anatomically based patient-specific finite element model of patella articulation: towards a diagnostic tool, Biomechan Model Mechanobiol (2005) 4: 20–38.
20. Bendjaballah MZ, Shirazi-Adl A, Zukor DJ (1995) Biomechanics of the human knee joint in compression: reconstruction, mesh generation and finite element analysis. Knee 2(2):69–79.
21. Drexler M, Dwyer T, Dolkart O, Goldstein Y, Steinberg EL, Chakravertty R, Cameron JC, Tibial rotational osteotomy and distal tuberosity transfer for patella subluxation secondary to excessive external tibial torsion: surgical technique and clinical outcome. Knee Surg Sports Traumatol Arthrosc,2014, 22(11): 2682–2689.
22. Catelas I, A M. New insights into wear and biological effects of metal-on-metal bearings. *The Journal of bone and joint surgery.* 2011;93(Suppl 2):76–83.
23. Yan Y, Neville A, Dowson D. Biotribocorrosion-an appraisal of the time dependence of wear and corrosion interactions: I. The role of corrosion. *J Phys D Appl Phys.* 2006a;39:200–205.
24. Alfons Fischer, Sabine Weiß, Markus A. Wimmer, The Tribological Difference between Biomedical Steels and CoCrMo-Alloys, J O U R N A L O F T H E M E C H A N I C A L B E H A V I O R O F B I O M E D I C A L M A T E R I A L (2 0 1 2); 5 0 – 6 2.
25. Paiva M, Blønd L, Hölmich P, Steensen RN, Diederichs G, Feller JA, Barfod KW , Quality assessment of radiological measurements of trochlear dysplasia; a literature review. Knee Surg Sports Traumatol Arthrosc,2017, https:// doi.org/10.1007/s00167-017-4520-z

26. Nwachukwu BU, So C, Schairer WW, Green DW, Dodwell ER, Surgical versus conservative management of acute patellar dislocation in children and adolescents: a systematic review. Knee Surg Sports Traumatol Arthrosc,2016, 24(3): 760–767.
27. Song G-Y, Hong L, Zhang H, Zhang J, Li X, Li Y, Feng H,Trochleoplasty versus nontrochleoplasty procedures in treating patellar instability caused by severe trochlear dysplasia. Arthroscopy,2014, 30(4):523 –532.
28. Dejour D, Le Coultre B. Osteotomies in patello-femoral instabilities. Sports Med Arthrosc. 2007;15:39–46.
29. Camp CL, Stuart MJ, Krych AJ, Levy BA, Bond JR, Collins MS, Dahm DL. CT and MRI measurements of tibial tubercle-trochlear groove distances are not equivalent in patients with patellar instability. Am J Sports Med 2013; 41: 1835-1840.
30. Wagner D, Pfalzer F, Hingelbaum S, Huth J, Mauch F, Bauer G,The influence of risk factors on clinical outcomes following anatomical medial patellofemoral ligament (MPFL) reconstruction using the gracilis tendon. Knee Surg Sports Traumatol Arthrosc,2013, 21(2):318 –324.
31. Wang S-n, C-h Q, Jiang N, Wang B-w, Wang L, Yu B, Is surgical treatment better than conservative treatment for primary patellar dislocations? A meta-analysis of randomized controlled trials. Arch Orthop Trauma Surg,2016, 136(3):371 –379.
32. Beaufls P, Thaunat M, Pujol N, Schefer S, Rossi R, Carmont M, Trochleoplasty in major trochlear dysplasia: current concepts. Sports Med Arthrosc Rehabil Ther Technol, 2012, 4:7.
33. Biedert RM, Lengthening osteotomy with or without elevation of the lateral trochlear facet. In: Dejour D, Zafagnini S, Arendt EA, Sillanpää P, Dirisamer F (eds) Patellofemoral pain, instability, and arthritis. Springer, Berlin, Heidelberg, 2020.

Published papers:

1. **Georgian Iacobescu**, Cătălin Cîrstoiu, Adrian Cursaru, Dan Anghelescu, Dumitru Stănculescu. Functional outcome and prognostic implications in patellofemoral instability using Elmslie-Trillat and MPFL reconstruction procedures. Romanian Journal of Orthopaedic Surgery and Traumatology. July-December 2019; 2(2):75-83. doi:10.2478/rojost-2019-0016.
2. **G. IACOBESCU**, C. CIRSTOIU, A. CURSARU, D. ANGHELESCU, D. STANCULESCU. Correlation between Patellar Tilt Angle, Femoral Anteversion and Tibial Tubercle Trochlear Groove Distance Measured by Computer Tomography in Patients with non-Traumatic Recurrent Patellar Dislocation. MAEDICA – a Journal of Clinical Medicine. 2020; 15(2):174-180. https://doi.org/10.26574/maedica.2020.15.2.174.
3. **Georgian Iacobescu**, Adrian Cursaru, Dan Anghelescu, Mihnea Popa, Dan Popescu. Correlations between intra and extraarticular factors measured by computed tomography in patients with recurrent patellar dislocation. Romanian Journal of Orthopaedic Surgery and Traumatology. January-June 2020; 3(1):20-28.